T. Shirasaki *et al.*	La protein required for internal ribosome entry site-directed translation is a potential therapeutic target for hepatitis C virus replication.	J Infect Dis.	202	75-85	2010
N. Arnaud *et al.*	Hepatitis C virus controls interferon production through PKR activation.	PLoS One	5	e10575	2010
A. Murayama *et al.*	RNA polymerase activity and specific RNA structure are required for efficient HCV replication in cultured cells.	PLoS Pathog.	6	e1000885	2010
T. Masaki *et al.*	Production of infectious hepatitis C virus by using RNA polymerase I-mediated transcription.	J Virol.	84	5824-5835	2010
K. Moriishi *et al.*	Involvement of PA28gamma in the propagation of hepatitis C virus.	Hepatology	52	411-420	2010
L. Yang *et al.*	Inhibitory effects on HAV IRES-mediated translation and replication by a combination of amantadine and interferon-alpha.	Virol J.	7	212	2010
Y. Zhang *et al.*	A novel function of CD81 in controlling hepatitis C virus replication.	J Virol.	84	3396-3407	2010
Y. Matsumoto *et al.*	Peripheral blood CD4 CD8 double-positive T cells of rhesus macaques become vulnerable to Simian Immunodeficiency Virus by *in vitro* stimulation due to the induction of CCR5.	J Vet Med Sci.	72	1057-1061	2010
T. Naruse *et al.*	Diversity of MHC class I genes in Burmese-origin rhesus macaques.	Immunogenetics	62	601-611	2010
T. Yoshida *et al.*	Characterization of natural killer cells in tamarins: a technical basis for studies of innate immunity.	Frontiers in Microbiology	1	128	2010
H. Oshiumi *et al.*	The ubiquitin ligase Riplet is essential for RIG-I-dependent innate immune responses to RNA virus infection.	Cell Host & Microbe	8	496-509	2010
H. Oshiumi *et al.*	Hepatitis C virus core protein abrogates the DDX3 function that enhances IPS-1-mediated IFN-b induction.	Plos ONE	5	e14258	2010
T. Ebihara *et al.*	Identification of a poly I:C-inducible membrane protein that participates in dendritic cell-mediated natural killer cell activation.	J Exp Med.	207	2675-2687	2010
M. Azuma *et al.*	The peptide sequence of diacyl lipopeptides determines dendritic cell TLR2- mediated NK activation.	Plos ONE	5	e12550	2010
M. Tatematsu *et al.*	A molecular mechanism for Toll/IL-1 receptor domain-containing adaptor molecule-1-mediated IRF-3 activation.	J Biol Chem.	285	20128-20136	2010

T. Akazawa *et al.*	Adjuvant engineering for cancer immunotherapy: development of a synthetic TLR2 ligand with increased cell adhesion.	Cancer Sci.	101	1596-1603	2010
H. Oshiumi *et al.*	DEAD/H BOX 3 (DDX3) helicase binds the RIG-I adaptor IPS-1 to up-regulate IFN-β inducing potential	Eur J Immunol.	40	940-948	2010
S. Hazari et al.	Impaired antiviral activity of interferon alpha against hepatitis C virus 2a in Huh-7 cells with a defective Jak-Stat pathway.	Virol J.	7	36	2010
M. Ishibashi et al.	2',5'-Oligoadenylate synthetase-like gene highly induced by hepatitis C virus infection in human liver is inhibitory to viral replication in vitro.	Biochem Biophys Res Commun.	392	397-402	2010
S. Hmwe et al.	Identification of hepatitis C virus genotype 2a replicon variants with reduced susceptibility to ribavirin.	Antiviral Res.	85	520-524	2010
X. Liu et al.	Systematic identification of microRNA and messenger RNA profiles in hepatitis C virus-infected human hepatoma cells.	Virology	398	57-67	2010
A. Angus et al.	Requirement of cellular DDX3 for hepatitis C virus replication is unrelated to its interaction with the viral core protein.	J Gen Virol.	91	122-132	2010

Ⅳ．研究成果の刊行物・別冊

Biochemical and Biophysical Research Communications 395 (2010) 565–571

Contents lists available at ScienceDirect

Biochemical and Biophysical Research Communications

journal homepage: www.elsevier.com/locate/ybbrc

Biological properties of purified recombinant HCV particles with an epitope-tagged envelope

Hitoshi Takahashi [a,b], Daisuke Akazawa [a,b], Takanobu Kato [a], Tomoko Date [a], Masayuki Shirakura [a,b], Noriko Nakamura [b], Hidenori Mochizuki [b], Keiko Tanaka-Kaneko [c], Tetsutaro Sata [c], Yasuhito Tanaka [d], Masashi Mizokami [e], Tetsuro Suzuki [a], Takaji Wakita [a,*]

[a] Department of Virology II, National Institute of Infectious Diseases, Tokyo, Japan
[b] Toray Industries, Inc., Kanagawa, Japan
[c] Department of Pathology, National Institute of Infectious Diseases, Tokyo, Japan
[d] Department of Clinical Molecular Informative Medicine, Nagoya City University Graduate School of Medicine, Nagoya, Japan
[e] Research Center for Hepatitis & Immunology, Kohnodai Hospital, International Medical Center of Japan, Chiba, Japan

ARTICLE INFO

Article history:
Received 3 April 2010
Available online 23 April 2010

Keywords:
Hepatitis C virus
Envelope protein
Purification
Particle
Vaccine

ABSTRACT

To establish a simple system for purification of recombinant infectious hepatitis C virus (HCV) particles, we designed a chimeric J6/JFH-1 virus with a FLAG (FL)-epitope-tagged sequence at the N-terminal region of the E2 hypervariable region-1 (HVR1) gene (J6/JFH-1/1FL). We found that introduction of an adaptive mutation at the potential *N*-glycosylation site (E2N151K) leads to efficient production of the chimeric virus. This finding suggests the involvement of glycosylation at Asn within the envelope protein(s) in HCV morphogenesis.

To further analyze the biological properties of the purified recombinant HCV particles, we developed a strategy for large-scale production and purification of recombinant J6/JFH-1/1FL/E2N151K. Infectious particles were purified from the culture medium of J6/JFH-1/1FL/E2N151K-infected Huh-7 cells using anti-FLAG affinity chromatography in combination with ultrafiltration. Electron microscopy of the purified particles using negative staining showed spherical particle structures with a diameter of 40–60 nm and spike-like projections. Purified HCV particle-immunization induced both an anti-E2 and an anti-FLAG antibody response in immunized mice. This strategy may contribute to future detailed analysis of HCV particle structure and to HCV vaccine development.

1. Introduction

The hepatitis C virus (HCV) causes chronic hepatitis, liver cirrhosis and hepatocellular carcinoma [1]. HCV is a positive strand RNA virus belonging to the *Hepacivirus* genus in the Flaviviridae family. The HCV genome consists of about 9600 nucleotides and contains three regions: a 5′ non-coding region of 341 nucleotides containing the sequence for the IRES structure, a coding region of about 9000 nucleotides, which encodes about 10 viral proteins, and a 3′ non-coding region of about 200 nucleotides depending on the size of the poly-uridylate track within this region [2,3].

The main therapy for HCV is treatment with pegylated-interferon and rivabirin. However, these agents show little effect in patients that have a high titer of HCV RNA, genotype 1. Thus, it is necessary to develop new, more effective therapies and preventive treatments to counteract HCV infection. As yet, no preventive vaccine is available for HCV. A recombinant HCV vaccine based on the viral envelope protein E1/E2 has been reported that generated neutralizing antibodies (nAb) in animals [4]. These nAbs were capable of limiting HCV pseudoparticles (HCVpp) and HCV cell culture (HCVcc) infection.

Recently, a genotype 2a strain of HCV named JFH-1 was discovered. This strain can efficiently replicate in the Huh-7 cell line [5], and an *in vitro* culture system of infectious HCV has also been successfully developed using the JFH-1 genome [6–8]. The JFH-1 viral production system is expected to become a powerful tool for HCV vaccine development. In this study, we developed a simple strategy for purification of recombinant HCV particles from the media of infected Huh-7 cells for structural analysis and for vaccine development using the JFH-1 genome.

2. Materials and methods

2.1. Plasmids

Plasmid pJ6/JFH-1 was generated from pJFH-1 by replacement of the 5′ untranslated region with the p7 region of J6 [9]. The

* Corresponding author. Address: Department of Virology II, National Institute of Infectious Diseases, 1-23-1 Toyama, Shinjuku, Tokyo 162-8640, Japan. Fax: +81 3 5285 1161.
E-mail address: wakita@nih.go.jp (T. Wakita).

0006-291X/$ - see front matter © 2010 Elsevier Inc. All rights reserved.
doi:10.1016/j.bbrc.2010.04.081

plasmids pJ6/JFH-1/1FL and pJ6/JFH-1/3FL were constructed by introduction of a single (DYKDDDDKGGG) or triple (DYKDHDG-DYKDHDIDYKDDDDKGGG) FLAG-tag sequence, respectively, into pJ6/JFH-1, which replaced part of the E2 HVR1 (amino acids 394–400) region. These two plasmids were then modified by introduction of a Lys residue to replace the Asn at amino acid position 151 of the E2 sequence, creating pJ6/JFH-1/1FL/E2N151K and pJ6/JFH-1/3FL/E2N151K, respectively.

The J6E2 gene (codons 1490–2500) was generated by PCR amplification from pJ6CF. The sense and antisense primers used were: 5′-CACAAGCTTCGCACCCATACTGTTGGGG-3′ and 5′-ACAGGATCCCAT-CGGACGATGTATTTTGTG-3′, respectively. For cloning purposes, HindIII or BamHI sites (underlined) were added to the primers. The amplified DNA was digested and inserted into p3XFLAG-CMV-13 (SIGMA, Saint Louis, MO).

The plasmid CDM-J6E2Fc encodes the J6E2 sequence downstream of the preprotrypsin leader sequence. pCDM-J6E2Fc was digested with SacI and BamHI, and the DNA fragment containing the preprotrypsin leader and J6E2 sequence was inserted into pCD4Rg (a kind gift from Dr. Brian Seed, Harvard Medical School) from which the SacI–BamHI fragment containing the CD4 gene was removed. This ligation resulted in the creation of a plasmid encoding a fusion gene of E2 and human IgG1-Fc.

2.2. Cell culture

The human hepatoma cell line, Huh-7, was maintained in DMEM supplemented with 10% FBS at 37 °C in a 5% CO_2 incubator.

2.3. In vitro synthesis of HCV RNA and RNA transfection of Huh cells

HCV RNA was synthesized from the plasmids described above *in vitro* using a MEGAscript T7 kit (Ambion, Austin, TX). Synthesized HCV RNA was then electroporated into cells as previously described [10]. The transfected cells were transferred onto 100-mm culture dishes containing culture medium.

2.4. Quantification of HCV core protein and RNA

The HCV core protein in cell culture supernatants or in purified HCV samples was quantified by enzyme immunoassay using a HCV core ELISA kit (Ortho Clinical Diagnostics). HCV RNA in purified HCV samples was quantified by RTD-PCR as previously described [11].

2.5. Deglycosylation with PNGase F

For deglycosylation reactions, the Enzymatic In-Solution N-Deglycosylation kit (Sigma) was used according to the manufacturer's instructions. Briefly, lysates of passaged cells were incubated for 10 min at 100 °C in denaturation buffer and then in the presence of PNGase F enzyme for 1 h at 37 °C. These samples were analyzed by Western blotting as described below using anti-FLAG (SIGMA) and anti-GAPDH (CHEMICON, Temecula, CA) antibodies.

2.6. Sequence analysis

The cDNAs of the HCV genome were synthesized from total RNA isolated from HCV RNA-transfected cells [5]. These cDNA were subsequently amplified using DNA polymerase (*TaKaRa LA Taq*, Takara, Shiga, Japan). The sequence of the amplified DNA was determined by the 3130 Genetic Analyzer (Applied Biosystems, Foster city, CA).

2.7. Purification of recombinant HCV particles

Culture supernatants from Huh-7 cells transfected with FLAG-tagged HCV RNA were harvested. The medium was concentrated by ultrafiltration using the pellicon-2 300 system (Millipore, Bedford, MA) and was subjected to affinity chromatography using an Anti-FLAG M2 affinity gel (Sigma). Virus particles were eluted using the 3×FLAG Peptide (Sigma) and were concentrated by ultracentrifugation for 2 h at 50,000 rpm at 4 °C.

2.8. Determination of the viral infectious titer

The infectious titer was determined by the method as previously described and was expressed as the number of focus-forming units per milliliter (FFU/mL) [6].

2.9. Western blotting

The purified HCV sample was lysed using a buffer containing 0.1 M Tris–HCl (pH 6.8), 4% SDS, 1.2% 2-mercaptoethanol, 20% glycerol, and Bromophenol blue. SDS–PAGE and immunoblotting were performed as previously described [6]. Antibodies used for immunoblotting were: anti-HCV core (clone 2H9) [6], anti-E1 (B7567) [6], and anti-E2 (clone 8D10-3, unpublished).

2.10. Electron microscopy

Concentrated, purified HCV particles were allowed to settle on carbon-coated copper grids and were stained with 4% uranylacetate. The grids were examined in a transmission electron microscope (H-7650, Hitachi, Tokyo, Japan) and were photographed at an instrumental magnification of 50,000×.

2.11. Sucrose density gradient analysis

The purified HCV sample containing 266 fmol of the HCV core was layered on a stepwise sucrose gradient (10–60%, wt/vol) and was centrifuged for 16 h in an SW41 rotor (Beckman Coulter, Fullerton, CA) at 35,000 rpm at 4 °C. After centrifugation, 12 fractions were harvested from the bottoms of the tubes. For each fraction, the core protein concentration was determined using an immunoassay. The HCV RNA titer was determined using RTD-PCR. The infectious titer was determined using an immunofluorescence assay as described above.

2.12. HCV particle-immunization

The purified HCV particles described above were inactivated by UV-irradiation, and 2 pmol of the HCV core protein of the particles were intraperitoneally injected into 4 week old BALB/c female mice ($n = 3$). Immunization was repeated four times at 2-week intervals (0, 2, 4 and 6 weeks). The Sigma Adjuvant System (Sigma), composed of monophosphoryl lipid A and trehalose dicorynomycolate, was used as an adjuvant. Saline alone was injected into control mice. Sera were collected at 1, 3, 5 and 7 weeks after immunization.

2.13. EIA for measurement of anti-E2 and anti-FLAG antibody responses

Recombinant J6E2/Fc or the FLAG peptide antigen (Sigma) was bound to microtiter plates (Nunc, Rochester, NY, USA) overnight at 4 °C, at a concentration of 50 ng per well. Recombinant J6E2/Fc was produced from COS-1 cells transfected with the CDM-J6E2Fc plasmid, which encodes the J6CF-E2 region (aa 384–720) fused with the Fc region of human IgG. The plates were blocked with Blocking One solution (Nacalai Tesque, Kyoto, Japan) and were washed with PBS containing 0.05% Tween 20 (washing buffer). Serum samples were diluted in washing buffer and were transferred to the blocked, antigen coated plates. After a 1.5-h incubation,

the plates were washed and bound antibody was detected using an HRP-conjugated anti-mouse antibody (GE healthcare, Buckinghamshire, England) and 3,3′,5,5′-tetramethylbenzidine (TMBZ) as a substrate (Sumitomo Bakelite, Tokyo, Japan).

3. Results

3.1. Production of recombinant HCV with an epitope-tagged envelope

To facilitate purification of recombinant HCV particles secreted into the culture medium of transfected cells, we constructed recombinant HCV with a FLAG-epitope-tagged envelope, which could then be purified by affinity chromatography using an anti-FLAG-agarose column. The FLAG-tagged HCV genome J6/JFH-1/3FL with the J6CF structural region was constructed by introducing a triple FLAG-tag sequence into the HVR1 of E2 (Fig. 1A). This region was selected for epitope-tag insertion because we predicted that this region would lie on the outside of the virus particles and would be tolerant to amino acid changes. Recombinant HCV particles were produced following transfection of Huh-7 cells with viral RNA, and were secreted into the culture medium.

RNA-transfected cells were passaged every 4 or 5 days. The level of the HCV core protein in the culture supernatant was measured over a period of 70 days (Fig. 1B). In contrast to the gradually increasing level of the core protein in J6/JFH-1 cells over time, the level of the core protein in the supernatants of the J6/JFH-1/3FL RNA-transfected cells decreased over the first 3 weeks post-transfection. Subsequently, the level began to increase and this level became equal to that of the wild-type J6/JFH-1 RNA-transfected cells 35 days post-transfection. This result suggested that after the first 35 days of culture, some mutations were introduced into the HCV genome that conferred efficient virus production during genome replication and/or that the transfected cells were altered in some way that was more favorable for viral production.

3.2. An N151K mutation facilitates the production of FLAG-tagged HCV

To determine if any adaptive mutations had arisen in the viral genome, we sequenced the full length of the HCV genome on days 8 and 35 post-J6/JFH-1/3FL RNA transfection. On day 8 post-transfection, no non-synonymous mutations were detected. However, on day 35, we found a single amino acid mutation at a potential

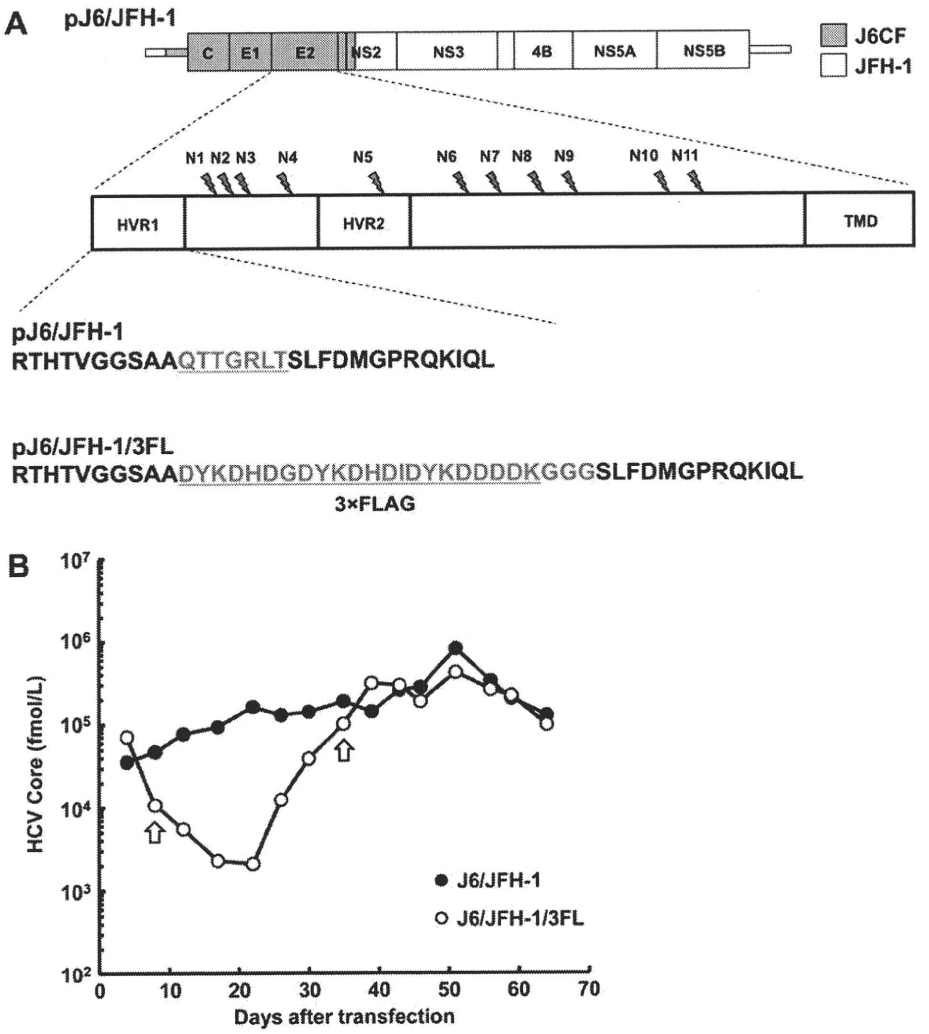

Fig. 1. Time course of HCV core protein secretion in recombinant HCV RNA-transfected cells. (A) Organization of the recombinant HCV construct pJ6/JFH-1/3FL. Open reading frames (thick boxes) are flanked by 5′- and 3′-UTRs (thin boxes). Gray, J6CF; white, JFH-1; HVR, hyper variable region; TMD, transmembrane domain. *N*-Glycosylation sites are indicated by pointers and are numbered N1–N11. The region of pJ6/JFH-1 that is replaced by the 3×FLAG sequence to generate pJ6/JFH-1/3FL is indicated at bottom. (B) HCV core protein secretion into the culture medium after HCV RNA transfection of Huh-7 cells. The HCV core protein was analyzed using an ELISA. Arrows indicate the times at which the J6/JFH-1/3FL HCV genome transfected into HCV RNA-transfected cells was sequenced.

N-glycosylation site of the E2 protein (Fig. 2A) in which asparagine at amino acid position 151 in the E2 protein was changed to lysine (E2N151K). Interestingly, this mutation was identical to that described by Delgrange et al. [12] as a mutation that was important for efficient production of HCV JFH-1. We performed Western blot analysis of cell lysates of transfected cells of different passages, using the anti-FLAG antibody as a probe for E2, to confirm that the N151K mutation abolishes one specific *N*-glycosylation. Indeed, the size of the FLAG-E2 protein was smaller on days 30 and 43 compared to that on day 4 (Fig. 2B). In contrast, the size of FLAG-E2 proteins that were deglycosylated using PNGase F was similar for all of the tested samples (Fig. 2B). This result suggested that the E2N151K mutation abolished *N*-glycosylation at this residue.

To investigate if the E2N151K mutation enhances production of FLAG-tagged HCV, we introduced the E2N151K mutation into the J6/JFH-1/3FL genome (J6/JFH-1/3FL/E2N151K). J6/JFH-1/3FL/E2N151K RNA-transfected cells were then passaged every 4 or 5 days and the level of the HCV core protein in the culture supernatant was measured over a period of 16 days (Fig. 2C). The result clearly showed that the E2N151K mutation contributes to efficient production of FLAG-tagged HCV particles.

We further analyzed the effect of the E2N151K mutation on specific viral infectivity (Table 1). The culture supernatant on day 3 post-transfection of recombinant viral RNA was therefore concentrated by ultrafiltration and tested in an infectious assay. The recombinant virus with the E2N151K mutation exhibited higher specific infectivity than the virus without this mutation. These data suggest that efficient production of infectious particles is impaired by the introduction of a FLAG-tag into the E2 protein but that this deficiency could be compensated for by the introduction of the E2N151K mutation which modifies an *N*-glycosylation site.

3.3. Purification of FLAG-tagged HCV

To purify FLAG-tagged HCV particles, we used a viral construct with a single FLAG-tag, J6/JFH-1/1FL/E2N151K (Fig. 1A), which as efficient in virus production as J6/JFH-1/3FL/E2N151K (data not shown). A total of 10 L of the culture supernatant of Huh-7 cells infected with J6/JFH-1/1FL/E2N151K was collected. This culture medium was concentrated to 300 mL by ultrafiltration and was then subjected to affinity chromatography using an anti-FLAG-agarose column. Bound virus particles were eluted using 10 mL of a

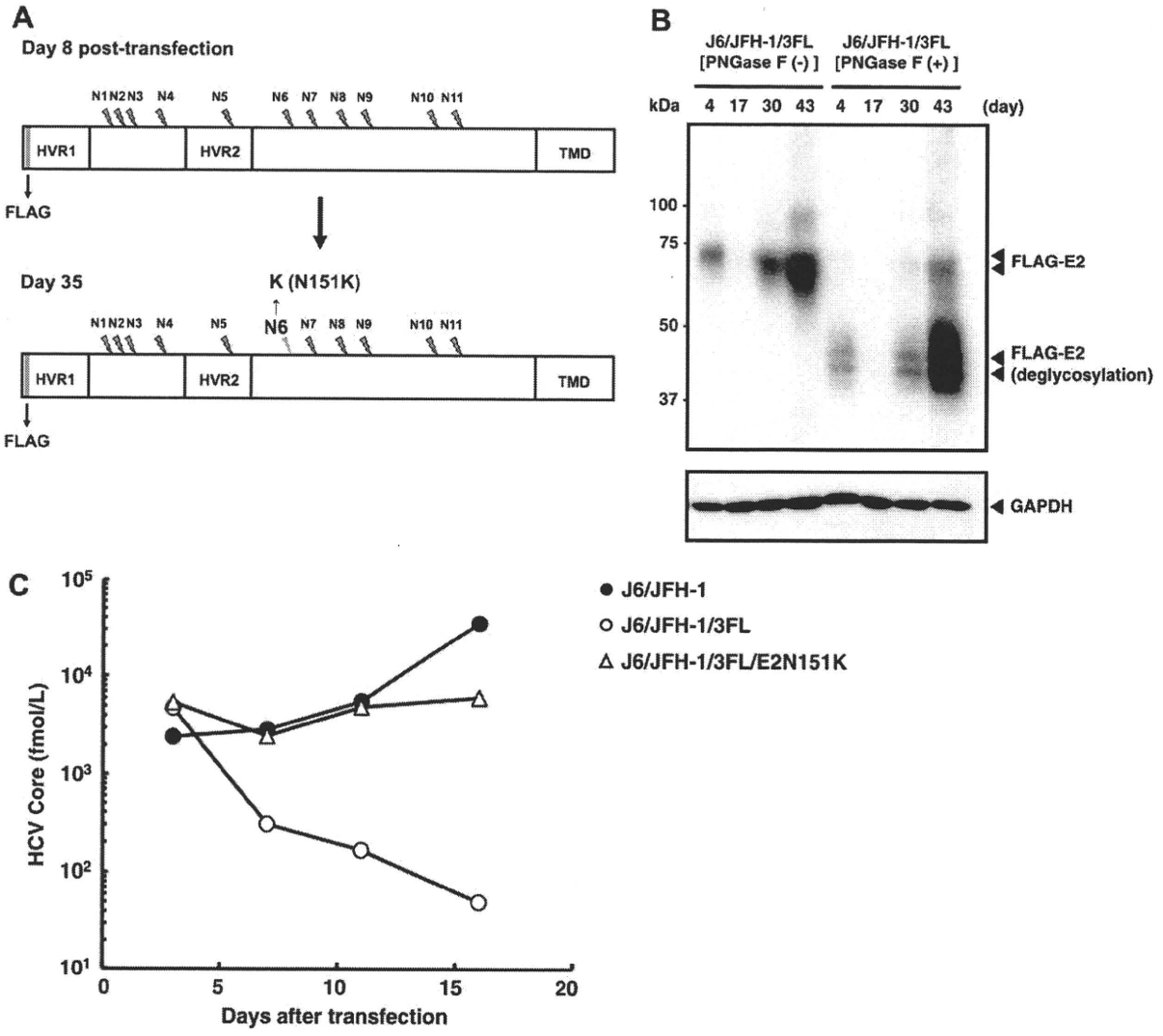

Fig. 2. Characterization of the recombinant HCV genome with an introduced N151K mutation. (A) Schematic diagram of the sequence of the E2 in the J6/JFH-1/3FL HCV RNA-transfected cells on day 8 and day 35 post-transfection. N151K replaces an Asn residue with a Lys residue at the N6 glycosylation site of E2. (B) Western blot analysis of the FLAG-E2 protein in lysates of cells transfected with J6/JFH-1/3FL RNA. Arrowheads indicate intact, and deglycosylated (PNGase F (+)), FLAG-E2 protein (upper panel) and control GAPDH protein (lower panel). (C) HCV core protein secretion into the culture medium following transfection of Huh-7 cells with HCV RNA with or without an introduced N151K mutation.

Table 1
Infectivity of recombinant viruses with or without N151K mutation.

Recombinant virus	Infectious titer ($\times 10^2$ FFU/mL)	HCV core protein ($\times 10^2$ fmol/mL)	Specific infectivity (FFU/HCV core)
J6/JFH-1/3FL	<1.7	1.6	<1.1
J6/JFH-1/3FL/E2N151K	8.3	2.0	4.2

FLAG peptide solution. Finally, the purified HCV particles were concentrated by ultracentrifugation.

The HCV yield and the amount of total protein after each purification step are summarized in Table 2. This purification process resulted in a 5000-fold concentration of the culture supernatant. The recovery of the HCV core protein in the final purified virus preparation was approximately 5%, and the virus purity was increased about 9000-fold compared to its purity in the initial culture medium. Specific infectivity was increased about 4-fold after the final step.

HCV structural proteins in the purified virus sample were examined by Western blotting (Fig. 3A). Core, E1 and E2 proteins were all detected in the purified virus preparation. Interestingly, incorporation of the E2 protein into the purified virus appeared to increase compared to incorporation of the core and E1 proteins. However, this higher apparent incorporation of FLAG-E2, may reflect the presence of free, non-virus incorporated FLAG-E2 proteins that co-purified with the FLAG-tagged virus. We further analyzed the virus particles in the purified preparation by electron microscopy (Fig. 3B–D). Substantial debris was found in the culture

Table 2
HCV yield and properties of purified recombinant HCV after each purification step.

Purification step	Volume (mL)	HCV core protein ($\times 10^2$ fmol/mL)	HCV RNA ($\times 10^7$ copies/mL)	Total protein (μg/mL)	Recovery[a] (%)	Purity[b]	Infectivity ($\times 10^2$ FFU/mL)	Specific infectivity (FFU/HCV core)
Culture supernatant	10,000	1.4	3.5	877	100	1	25	18
Concentrate (after Ultrafiltration)	300	45	57	19,597	96	0.73	743	17
Affinity purification (after Elution)	10	98	324	171	7	469	4240	43
Concentrate (after Ultracentrifugation)	0.2	1440	3220	84	5	9546	94,600	66

[a] Recovery of HCV core protein.
[b] The degree of virus purity was calculated by HCV RNA contents per μg total proteins.

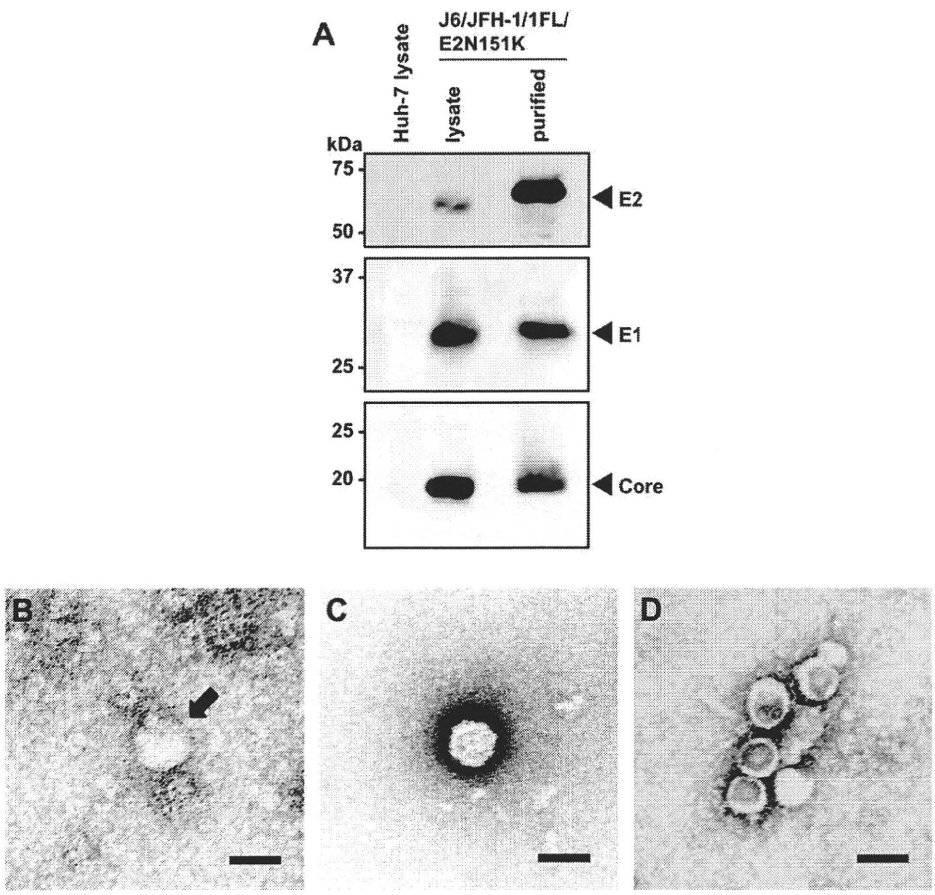

Fig. 3. Analysis of purified HCV particles. (A) Western blot analysis of viral proteins in lysates of, and in HCV particles purified from, whole-cell extracts of Huh-7 cells transfected with J6/JFH-1/1FL N151K RNA. Lysates of non-transfected cells were also analyzed. The arrowheads indicate the positions of the HCV core, E1 and E2 proteins. Marker proteins are shown at left. (B–D) Electron micrographs using negative staining of: (B) An HCV particle from culture media (indicated by an arrow.), (C) A purified HCV particle and (D) Purified HCV particles aggregated by an anti-FLAG antibody. Scale bar, 50 nm.

supernatant concentrated by ultrafiltration, which made it difficult to identify virus particles (Fig. 3B). In contrast, spherical particle structures of 40–60 nm could be clearly observed in the purified samples (Fig. 3C and D). Furthermore, the purified FLAG-tagged HCV particles were aggregated by the anti-FLAG antibody (Fig. 3D). The size and morphology of the FLAG-tagged particles were similar to each other but with slight deviations. The combined data suggest that the FLAG-tagged HCV particles can be purified by affinity chromatography using anti-FLAG-agarose.

3.4. Physical properties of purified FLAG-tagged HCV

We next further analyzed the properties of the purified FLAG-tagged HCV particles. The total number of proteins in the purified viral sample, as judged by SDS–PAGE and silver staining analysis, was much lower than that in the original culture medium (Fig. 4A). We confirmed by mass spectrometry analysis that these extra protein bands in the purified preparation were not viral proteins but were host proteins that bound to the FLAG-agarose (data not shown).

We further analyzed the purified FLAG-tagged HCV particles using a sucrose density gradient (Fig 4B). Purified virus was layered on top of a preformed continuous 10–60% sucrose gradient and was then centrifuged. Twelve fractions were collected and the HCV core protein, RNA and viral infectivity were determined for each fraction. The HCV particles migrated at a density between 1.13 and 1.16 g sucrose/mL. The density at which the peak of the HCV core protein was observed was almost identical to the density at which the HCV RNA and infectivity were detected.

3.5. Immunogenicity of purified HCV particles

To examine the immunogenicity of the FLAG-tagged HCV particles, they were injected into BALB/c mice and the sera of these mice were then analyzed for reactivity with recombinant J6E2/Fc or the FLAG peptide using an ELISA. The HCV particles were inactivated by UV-irradiation prior to injection using the Sigma Adjuvant System as an adjuvant. Both anti-E2 and anti-FLAG antibodies were induced in mice sera after four immunizations (Fig. 4C). These results suggested that the envelope proteins of the FLAG-tagged HCV

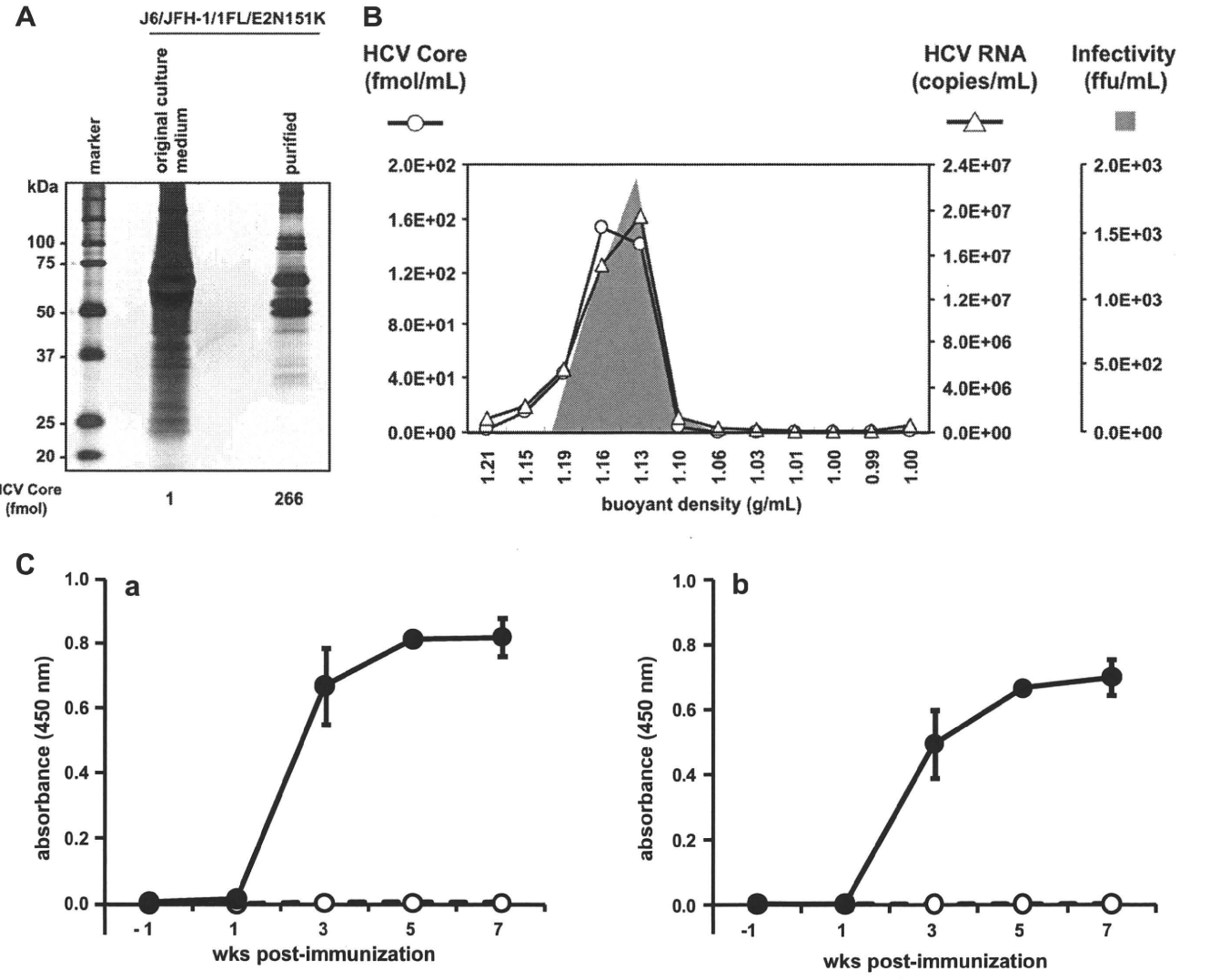

Fig. 4. Physical properties and immunogenicity of purified HCV particles. (A) Silver staining of non-purified (original culture medium) and purified HCV samples. The non-purified and purified samples contained 1 and 266 fmol, respectively, of the HCV core. (B) Sucrose density gradient analysis of purified HCV particles. The level of the HCV core protein (open circles), HCV RNA (open triangles) and the HCV infectivity towards naïve Huh-7 cells (shown in gray) were analyzed for each fraction as described in Section 2. (C) Purified HCV particles (closed circles) or saline (open circles) were intraperitoneally injected into BALB/c mice ($n = 3$), and sera were collected at the indicated times. The collected sera were examined for the presence of anti-E2 (a) and anti-FLAG (b) antibodies using the J6E2/Fc protein and the FLAG peptide as antigens in an EIA as described in Section 2.

particles were immunogenic and that insertion of a tag into the E2 protein could induce antibodies as a secondary immunogen.

4. Discussion

In this study we showed that infectious FLAG-tagged HCV particles with an N151K mutation that modulated HCV-glycosylation could be efficiently produced in cells and purified on a FLAG-agarose column. This purification procedure allowed analysis of the physical properties of the particles and the generation of anti-E2 antibodies.

The FLAG-tagged HCV particles were purified by simple anti-FLAG affinity chromatography in combination with ultrafiltration. However, the efficiency of purification was low, and the recovery of the HCV core protein in the final purified virus preparation was only approximately 5%. This low efficiency of purification of the HCV particles maybe due to a number of factors: (1) Interaction between the E2-FLAG protein and the anti-FLAG-agarose column may have been prevented by cellular host proteins with specific or non-specific affinity for the anti-FLAG-agarose, (2) A conformation change may have occurred in the E2 protein due to insertion of the FLAG sequence, which may have blocked FLAG interaction with anti-FLAG, (3) Free FLAG-E2 proteins may have bound more tightly to the FLAG-agarose than the FLAG-E2 protein on the viral surface. Nevertheless, sufficient purified FLAG-HCV particles were obtained with this purification procedure for further analysis.

In the density gradient analysis of the purified HCV particles, the peak of the HCV core protein coincided with the peaks of HCV RNA and viral infectivity. In previous reports of density gradient fractionation of non-FLAG-tagged viral particles, the peak of infectivity was reported to shift to a lighter density fraction than the peaks of HCV core protein or RNA [8,13,14]. This discrepancy between our, and previous, data may be explained by the fact that the properties of the purified FLAG-tagged HCV particles may differ from those of the JFH-1 based HCV particles reported previously. Regarding viral infectivity, it is known that cholesterol and sphingolipid association with HCV particles is important for virion maturation and infectivity [9]. The association of HCV particles with these lipids occurs in lipid rafts [9]. Since the E2-FLAG protein may have a decreased dependency on lipid rafts compared to the non-tagged E2 protein, this therefore resulted in a shift in the peak of infectivity. Alternatively, an association between HCV and very-low-density lipoprotein (VLDL) has an important role in HCV infectivity [15]. Tagging of HCV particles with FLAG may have somehow changed the association of HCV with VLDL and cause the observed shift in the infectivity peak. The mechanism of the shift of the infectivity peak of the FLAG-HCV particles needs to be examined in more detail in future studies.

HCV particles from human plasma samples have been previously examined by immunogold electron microscopy [16]. In the present study, we could clearly observe spherical particle structures of 40–60 nm in the purified samples. Furthermore, the FLAG-tagged HCV particles were aggregated by anti-FLAG antibody. This is the first report of the aggregation of HCV particles produced in an *in vitro* culture system. This method may therefore facilitate future examination of the detailed conformation of HCV particles and future elucidation of HCV particle structure by cryo-electron microscopy. However, it is regarded structural analysis as difficult to that aggregated HCV particles were inequable showing in this report because of this method also gathered defective viral particles which have the E2-FLAG protein.

Immunization of mice with purified FLAG-tagged HCV particles induced anti-E2 as well as anti-FLAG antibodies. These results indicated that the envelope proteins of the FLAG-tagged HCV particles were immunogenic and that insertion of a tag into the E2 protein could induce antibodies as a secondary immunogen. Thus, not only epitopes of viral origin, but also an epitope inserted into the virus, can induce an immune response. Although it is unclear how many amino acids can be inserted into the E2 HVR1, at least a triple FLAG-tag sequence (25 amino acids) is possible as shown in this study.

In conclusion, we have established a simple system for the purification of recombinant infectious FLAG-epitope-tagged HCV particles. The use of this system may contribute to studies aimed at a detailed analysis of HCV particle structure and towards HCV vaccine development.

Acknowledgments

This work was partially supported by a grant-in-aid for Scientific Research from the Japan Society for the Promotion of Science, from the Ministry of Health, Labor and Welfare of Japan, by the Research on Health Sciences Focusing on Drug Innovation from the Japan Health Sciences Foundation, and by the Japanese Society of Gastroenterology.

References

[1] K. Shimotohno, Hepatitis C virus as a causative agent of hepatocellular carcinoma, Intervirology 38 (1995) 162–169.
[2] Q.L. Choo, K.H. Richman, J.H. Han, K. Berger, C. Lee, C. Dong, C. Gallegos, D. Coit, R. Medina-Selby, P.J. Barr, A.J. Weiner, D.W. Bradley, G. Kuo, M. Houghton, Genetic organization and diversity of the hepatitis C virus, Proc. Natl. Acad. Sci. USA 88 (1991) 2451–2455.
[3] N. Kato, M. Hijikata, Y. Ootsuyama, M. Nakagawa, S. Ohkoshi, T. Sugimura, K. Shimotohno, Molecular cloning of the human hepatitis C virus genome from Japanese patients with non-A, non-B hepatitis, Proc. Natl. Acad. Sci. USA 87 (1990) 9524–9528.
[4] Z. Stamataki, S. Coates, M.J. Evans, M. Wininger, K. Crawford, C. Dong, Y.L. Fong, D. Chien, S. Abrignani, P. Balfe, C.M. Rice, J.A. McKeating, M. Houghton, Hepatitis C virus envelope glycoprotein immunization of rodents elicits cross-reactive neutralizing antibodies, Vaccine 25 (2007) 7773–7784.
[5] T. Kato, T. Date, M. Miyamoto, A. Furusaka, K. Tokushige, M. Mizokami, T. Wakita, Efficient replication of the genotype 2a hepatitis C virus subgenomic replicon, Gastroenterology 125 (2003) 1808–1817.
[6] T. Wakita, T. Pietschmann, T. Kato, T. Date, M. Miyamoto, Z. Zhao, K. Murthy, A. Habermann, H.G. Krausslich, M. Mizokami, R. Bartenschlager, T.J. Liang, Production of infectious hepatitis C virus in tissue culture from a cloned viral genome, Nat. Med. 11 (2005) 791–796.
[7] J. Zhong, P. Gastaminza, G. Cheng, S. Kapadia, T. Kato, D.R. Burton, S.F. Wieland, S.L. Uprichard, T. Wakita, F.V. Chisari, Robust hepatitis C virus infection in vitro, Proc. Natl. Acad. Sci. USA 102 (2005) 9294–9299.
[8] B.D. Lindenbach, M.J. Evans, A.J. Syder, B. Wolk, T.L. Tellinghuisen, C.C. Liu, T. Maruyama, R.O. Hynes, D.R. Burton, J.A. McKeating, C.M. Rice, Complete replication of hepatitis C virus in cell culture, Science 309 (2005) 623–626.
[9] H. Aizaki, K. Morikawa, M. Fukasawa, H. Hara, Y. Inoue, H. Tani, K. Saito, M. Nishijima, K. Hanada, Y. Matsuura, M.M. Lai, T. Miyamura, T. Wakita, T. Suzuki, Critical role of virion-associated cholesterol and sphingolipid in hepatitis C virus infection, J. Virol. 82 (2008) 5715–5724.
[10] M.J. van den Hoff, A.F. Moorman, W.H. Lamers, Electroporation in 'intracellular' buffer increases cell survival, Nucleic Acids Res. 20 (1992) 2902.
[11] T. Takeuchi, A. Katsume, T. Tanaka, A. Abe, K. Inoue, K. Tsukiyama-Kohara, R. Kawaguchi, S. Tanaka, M. Kohara, Real-time detection system for quantification of hepatitis C virus genome, Gastroenterology 116 (1999) 636–642.
[12] D. Delgrange, A. Pillez, S. Castelain, L. Cocquerel, Y. Rouille, J. Dubuisson, T. Wakita, G. Duverlie, C. Wychowski, Robust production of infectious viral particles in Huh-7 cells by introducing mutations in hepatitis C virus structural proteins, J. Gen. Virol. 88 (2007) 2495–2503.
[13] D. Akazawa, T. Date, K. Morikawa, A. Murayama, N. Omi, H. Takahashi, N. Nakamura, K. Ishii, T. Suzuki, M. Mizokami, H. Mochizuki, T. Wakita, Characterization of infectious hepatitis C virus from liver-derived cell lines, Biochem. Biophys. Res. Commun. 377 (2008) 747–751.
[14] Y. Miyanari, K. Atsuzawa, N. Usuda, K. Watashi, T. Hishiki, M. Zayas, R. Bartenschlager, T. Wakita, M. Hijikata, K. Shimotohno, The lipid droplet is an important organelle for hepatitis C virus production, Nat. Cell Biol. 9 (2007) 1089–1097.
[15] S.U. Nielsen, M.F. Bassendine, A.D. Burt, C. Martin, W. Pumeechockchai, G.L. Toms, Association between hepatitis C virus and very-low-density lipoprotein (VLDL)/LDL analyzed in iodixanol density gradients, J. Virol. 80 (2006) 2418–2428.
[16] M. Kaito, S. Watanabe, H. Tanaka, N. Fujita, M. Konishi, M. Iwasa, Y. Kobayashi, E.C. Gabazza, Y. Adachi, K. Tsukiyama-Kohara, M. Kohara, Morphological identification of hepatitis C virus E1 and E2 envelope glycoproteins on the virion surface using immunogold electron microscopy, Int. J. Mol. Med. 18 (2006) 673–678.

JOURNAL OF VIROLOGY, Nov. 2010, p. 11761–11770 Vol. 84, No. 22
0022-538X/10/$12.00 doi:10.1128/JVI.00638-10

Sphingomyelin Activates Hepatitis C Virus RNA Polymerase in a Genotype-Specific Manner▽†

Leiyun Weng,[1] Yuichi Hirata,[2] Masaaki Arai,[3] Michinori Kohara,[2] Takaji Wakita,[4] Koichi Watashi,[4,5] Kunitada Shimotohno,[5,6] Ying He,[7] Jin Zhong,[7] and Tetsuya Toyoda[1]*

Units of Viral Genome Regulation[1] and Viral Hepatitis,[7] Institut Pasteur of Shanghai, Key Laboratory of Molecular Virology and Immunology, Chinese Academy of Sciences, 411 Hefei Road, 200025 Shanghai, People's Republic of China; Department of Microbiology and Cell Biology, Tokyo Metropolitan Institute of Medical Biology, 3-18-22 Honkomagome, Bunkyo-Ku, Tokyo 113-8613, Japan[2]; Pharmacology Laboratory, Pharmacology Department V, Mitsubishi Tanabe Pharma Corporation, 1000 Kamoshida-cho, Aoba-ku, Yokohama 227-0033, Japan[3]; Department of Virology II, National Institute of Health, 1-23-1 Toyama, Shinjuku, Tokyo 132-8640, Japan[4]; Laboratory of Human Tumor Viruses, Department of Viral Oncology, Institute for Virus Research, Kyoto University, Kyoto 606-8507, Japan[5]; and Chiba Institute of Technology, 2-17-1 Tsudamuna, Narashino, Chiba 275-0016, Japan[6]

Received 25 March 2010/Accepted 27 August 2010

Hepatitis C virus (HCV) replication and infection depend on the lipid components of the cell, and replication is inhibited by inhibitors of sphingomyelin biosynthesis. We found that sphingomyelin bound to and activated genotype 1b RNA-dependent RNA polymerase (RdRp) by enhancing its template binding activity. Sphingomyelin also bound to 1a and JFH1 (genotype 2a) RdRps but did not activate them. Sphingomyelin did not bind to or activate J6CF (2a) RdRp. The sphingomyelin binding domain (SBD) of HCV RdRp was mapped to the helix-turn-helix structure (residues 231 to 260), which was essential for sphingomyelin binding and activation. Helix structures (residues 231 to 241 and 247 to 260) are important for RdRp activation, and 238S and 248E are important for maintaining the helix structures for template binding and RdRp activation by sphingomyelin. 241Q in helix 1 and the negatively charged 244D at the apex of the turn are important for sphingomyelin binding. Both amino acids are on the surface of the RdRp molecule. The polarity of the phosphocholine of sphingomyelin is important for HCV RdRp activation. However, phosphocholine did not activate RdRp. Twenty sphingomyelin molecules activated one RdRp molecule. The biochemical effect of sphingomyelin on HCV RdRp activity was virologically confirmed by the HCV replicon system. We also found that the SBD was the lipid raft membrane localization domain of HCV NS5B because JFH1 (2a) replicon cells harboring NS5B with the mutation A242C/S244D moved to the lipid raft while the wild type did not localize there. This agreed with the myriocin sensitivity of the mutant replicon. This sphingomyelin interaction is a target for HCV infection because most HCV RdRps have 241Q.

Hepatitis C virus (HCV) has a positive-stranded RNA genome and belongs to the family *Flaviviridae* (21). HCV chronically infects more than 130 million people worldwide (34), and HCV infection often induces liver cirrhosis and hepatocellular carcinoma (19, 28). To date, pegylated interferon (PEG-IFN) and ribavirin are the standard treatments for HCV infection. However, many patients cannot tolerate their serious side effects. Therefore, the development of new and safer therapeutic methods with better efficacy is urgently needed.

Lipids play important roles in HCV infection and replication. For example, the HCV core associates with lipid droplets and recruits nonstructural proteins and replication complexes to lipid droplet-associated membranes which are involved in the production of infectious virus particles (24). HCV RNA replication depends on viral protein association with raft membranes (2, 30). The association of cholesterol and sphingolipid with HCV particles is also important for virion maturation and infectivity (3). The inhibitors of the sphingolipid biosynthetic pathway, ISP-1 and HPA-12, which specifically inhibit serine palmitoyltransferase (SPT) (23) and ceramide trafficking from the endoplasmic reticulum (ER) to the Golgi apparatus (37), suppress HCV virus production in cell culture but not viral RNA replication by the JFH1 replicon (3). Other serine SPT inhibitors (myriocin and NA255) inhibit genotype 1b replication (4, 29, 33). Very-low-density lipoprotein (VLDL) also interacts with the HCV virion (15).

Sakamoto et al. reported that sphingomyelin bound to HCV RNA-dependent polymerase (RdRp) at the sphingomyelin binding domain (SBD; amino acids 230 to 263 of RdRp) to recruit HCV RdRp on the lipid rafts, where the HCV complex assembles, and that NA255 suppressed HCV replication by releasing HCV RdRp from the lipid rafts (29). In the present study, we analyzed the effect of sphingomyelin on HCV RdRp activity *in vitro* and found that sphingomyelin activated HCV RdRp activity in a genotype-specific manner. We also determined the sphingomyelin activation domain and the activation mechanism. Finally, we confirmed our biochemical data by a HCV replicon system.

MATERIALS AND METHODS

HCV RNA polymerase. A C-terminal 21-amino-acid deletion was made to the HCV RdRps of strains HCR6 (genotype 1b) (36), NN (1b) (35), Con1 (1b) (5), JFH1 (2a) (36), J6CF (2a) (25), H77 (1a) (7), and RMT (1a), and the mutants

* Corresponding author. Mailing address: Unit of Viral Genome Regulation, Institut Pasteur of Shanghai, Chinese Academy of Sciences, 411 Hefei Road, 200025 Shanghai, People's Republic of China. Phone and fax: 86 21 6385 1621. E-mail: ttoyoda@amber.plala.or.jp.

† Supplemental material for this article may be found at http://jvi.asm.org.

▽ Published ahead of print on 15 September 2010.

were purified from bacteria as described previously (36). HCR6 (1b) RdRp with the mutation L245A [RdRp(L245A)] or I253A [RdRp(I253A)] or the double mutation L245A and I253A [RdRp(L245A/I253A)]; JFH1 (2a) RdRp with the mutation(s) A242C/S244D, A242, S244D, or T251Q; J6CF (2a) RdRp with the mutation(s) R241Q, S244D, or R241Q/S244D; and H77 (1a) RdRp(A238S/Q248E) were introduced using an *in vitro* mutagenesis kit (Stratagene) and the oligonucleotides listed in Table S1 in the supplemental material. HCR6 (1b) His_6-tagged RdRp(L245A/I253A) was removed from pET21b/KM (36) and cloned into the BamHI/XhoI site of pGEX-6P-3 (GE), resulting in pGEXHCVHCR6RdRp(L245A/I253A).

***In vitro* HCV transcription.** *In vitro* HCV transcription was performed as described previously (36). Briefly, following 30 min of preincubation without ATP, CTP, or UTP, 100 nM HCV RdRp was incubated in 50 mM Tris-HCl (pH 8.0), 200 mM monopotassium glutamate, 3.5 mM $MnCl_2$, 1 mM dithiothreitol (DTT), 0.5 mM GTP, 50 μM ATP, 50 μM CTP, 5 μM [α-^{32}P]UTP, 200 nM RNA template (SL12-1S), 100 U/ml human placental RNase inhibitor, and the lipid (amount indicated below) at 29°C for 90 min. ^{32}P-labeled RNA products were subjected to 6% polyacrylamide gel electrophoresis (PAGE) containing 8 M urea. The resulting autoradiograph was analyzed with a Typhoon Trio plus image analyzer (GE).

RNA filter binding assay. An RNA filter binding assay was performed as described previously (36). Briefly, 100 nM HCV RdRp and 100 nM ^{32}P-labeled RNA template (SL12-1S) were incubated with or without 0.01 mg/ml egg yolk sphingomyelin in 25 μl of 50 mM Tris-HCl (pH 7.5), 200 mM monopotassium glutamate, 3.5 mM $MnCl_2$, and 1 mM DTT at 29°C for 30 min. After incubation, the solutions were diluted with 0.5 ml of TE (50 mM Tris-HCl [pH 7.5], 1 mM EDTA) buffer and filtered through nitrocellulose membranes (0.45-μm pore size; Millipore). The filter was washed five times with TE buffer, and the bound radioisotope was analyzed by Typhoon Trio plus after being dried.

Enzyme-linked immunosorbent assay (ELISA). Ninety-six-well microtiter plates (Corning) were coated with 250 ng of egg yolk sphingomyelin in ethanol by evaporation at room temperature. After the wells were blocked with phosphate-buffered saline (PBS) and 3% bovine serum albumin (BSA), they were incubated with 1 pmol of the HCV RdRp of HCR6 (1b) wild type (wt) or L245A, I253A, or L245A/I253A mutant; NN (1b); H77 (1a); RMT (1a); J6CF (2a); or JFH1 (2a) wt or A242C/S244D, A242, S244D, or T251Q mutant in Tris-buffered saline (50 mM Tris-HCl [pH 7.5] and 150 mM NaCl) for 1.5 h at room temperature. After being blocked with 3% BSA, the bound HCV RdRp was detected by adding rabbit anti-HCV RdRp serum (1:5,000) (see Fig. S1 in the supplemental material) (17) before incubation with a horseradish peroxidase (HRP)-conjugated anti-rabbit IgG antibody (1:5,000; Southern Biotech). The optical density at 450 nm (OD_{450}) was measured with a Spectra Max 190 spectrophotometer (Molecular Devices) using a TMB (3,3′,5,5′-tetramethylbenzidine) Liquid Substrate System (Sigma).

HCV subgenomic replicon. A D244S mutation was introduced into the HCV strain NN (1b) subgenomic replicon pLMH14 (35), resulting in pLMH(NN)5B(D244S) [where 5B(D244S) is the NS5B protein with the mutation D244S]. The A242C/S244D mutation was introduced into the HCV JFH1 (2a) replicon, pSGR-JFH1/luc (25), resulting in pSGR-JFH1/luc5B(A242C/S244D). The HpaI and XbaI fragment of pSGR-JFH1 (18) was replaced with that of pSGR-JFH1/luc5B(A242C/S244D), resulting in pSGR-JFH15B(A242C/S244D). The A238S/Q248E mutation was introduced into HCV H77 (1a) replicon pHCVrep13(S2204I)/Neo (7) after the neomycin gene was replaced by the firefly luciferase gene [pH77(I)/luc] by insertion of AflII and AscI sites (see Table S1 in the supplemental material), resulting in pH77(I)/luc5B(A238S/Q248E). Subgenomic replicon RNA was transcribed *in vitro* by T7 RNA polymerase using MegaScript (Ambion) after the replicon plasmids were linearized by XbaI (strain NN and JFH1 replicons) or HpaI (strain H77 replicon). Subgenomic replicon RNA was stored at −80°C after being purified by phenol-chloroform extraction and ethanol precipitation.

Replicon assay with myriocin. Huh7.5.1 cells were kindly provided by F. Chisari and were maintained in Dulbecco's modified Eagle's medium (DMEM; Gibco) with 10% fetal bovine serum (FBS; Gibco) (38). HCV replicon RNA (10 μg) was transfected into 4×10^6 Huh7.5.1 cells (1×10^7/ml) in OptiMEM I (Gibco) by electroporation (GenePulser Xcell; Bio-Rad) at 270 V, 100 Ω, and 950 μF. After transfection, the cells were plated in 12-well plates incubated in DMEM–10% FBS. At 6 h after transfection, cells were treated with 0, 5, and 50 nM myriocin. At 4, 54, and 78 h after transfection (48 and 72 h after myriocin treatment), the cells were harvested, and luciferase activity was measured using a Dual-Glo luciferase assay kit and a GloMax 96 Microplate Luminometer (Promega). Luciferase activity was normalized against the activity at 4 h after transfection (26).

HCV JFH1 wt and NS5B(A242C/S244D) replicon cells. Huh7/scr cells were kindly provided by F. Chisari of the Scripps Research Institute and were maintained in Dulbecco's modified Eagle's medium (Gibco) with 10% fetal bovine serum (Gibco). RNA (10 μg each) from SGR-JFH1 and SGR-JFH1 with the mutations A242C/S244D in NS5B [NS5B(A242C/S244D) was transfected into 4×10^6 Huh7/scr cells (1×10^7/ml) in OptiMEM I (GIBCO) by electroporation (GenePulser Xcell; Bio-Rad) at 270 V, 100 Ω, and 950 μF. After transfection, the cells were plated in 10-cm dishes and incubated in DMEM–10% FBS with 1.0 and 0.5 mg/ml G418 (Gibco). JFH1 wt and NS5B(A242C/S244D) replicon cells were maintained in DMEM–10% FBS and 0.5 mg/ml G418.

Membrane floating assay. JFH1 wt and NS5B(A242C/S244D) replicon cells were suspended in two packed cell volumes of hypotonic buffer (10 mM HEPES-NaOH [pH 7.6], 10 mM KCl, 1.5 mM $MgCl_2$, 2 mM DTT, and 1 tablet/25 ml of EDTA-free protease inhibitor cocktail tablets [Roche]) and disrupted by 30 strokes of homogenization in a Dounce homogenizer using a tight-fitting pestle at 4°C. After nuclei were removed by centrifugation at 2,000 rpm for 10 min at 4°C, the supernatant (postnuclear supernatant [PNS]) was treated with 1% Triton X-100 in TNE buffer (25 mM Tris-HCl [pH 7.6] 150 mM NaCl, 1 mM EDTA) for 30 min on ice. The lysates were supplemented with 40% sucrose and centrifuged at 38,000 rpm in a Beckman SW41 Ti rotor (Beckman Coulter) overlaid with 30% and 10% sucrose in TNE buffer at 4°C for 14 h.

Western blotting. Western blotting using anti-HCV RdRp (17), rabbit anti-NS3 (32), anti-NS5A (16) and anti-caveolin-2 was performed as previously published (17).

Reagent. Egg yolk sphingomyelin, cholesterol phosphocholine, myriocin, and rabbit anti-caveolin-2 antibodies were purchased from Sigma. Hexanoyl sphingomyelin, C_6-ceramide, C_8-β-D-glucosyl ceramide, and C_8-β-D-lactosyl ceramide were purchased from Avanti Polar Lipids. [α-^{32}P]UTP was purchased from New England Nuclear.

Statistical analysis. Significant differences were evaluated using *P* values calculated from a Student's *t* test.

Nucleotide sequence accession number. The sequence of HCV RMT has been deposited in the GenBank under accession number AB520610.

RESULTS

Sphingomyelin activation of HCV RNA polymerases of various genotypes. There are several sequence variations in the sphingomyelin binding domain (SBD; amino acids 231 to 260 of HCV RdRp) among HCV genotypes (see Fig. 7A). In order to compare the RdRps of different genotypes of HCV, we purified RdRp from genotypes 1b (strains HCR6, NN, and Con1), 1a (H77 and MRT), and 2a (JFH1 and J6CF) (see Fig. S2 in the supplemental material). First, the effect of ethanol on HCV HCR6 (1b) RdRp transcription was examined because lipids were suspended in ethanol before they were added to the HCV transcription reaction mixture. We found that 2% ethanol did not inhibit HCV transcription (see Fig. S3 in the supplemental material); therefore, all subsequent experiments were performed using less than 2% ethanol.

The kinetics of sphingomyelin activation were analyzed using egg yolk sphingomyelin for HCR6 (1b) RdRp wt (Fig. 1A) and subtype 2a (JFH1 and J6CF) RdRps (Fig. 1B), and *N*-hexanoyl-D-*erythro*-sphingosylphosphorylcholine (hexanoyl sphingomyelin) was used for HCR6 (1b) RdRp wt (Fig. 1C) and subtype 1a (H77 and RMT) RdRps (Fig. 1D). The egg yolk sphingomyelin activation curve of HCR6 (1b) RdRp wt at low concentrations (<0.01 mg/ml) was sigmoid. The transcription activity of HCR6 (1b) RdRp wt increased in a dose-dependent manner. It was activated 11-fold at 0.01 mg/ml and then plateaued (14-fold activation) at 0.1 mg/ml. However, JFH1 (2a) and J6CF (2a) RdRps were activated 2.5-fold and 2.2-fold, respectively, at 0.01 mg/ml sphingomyelin, at which point they plateaued.

Egg yolk sphingomyelin is a mixture. In order to obtain the optimal molar ratio for sphingomyelin activation of HCR6 (1b)

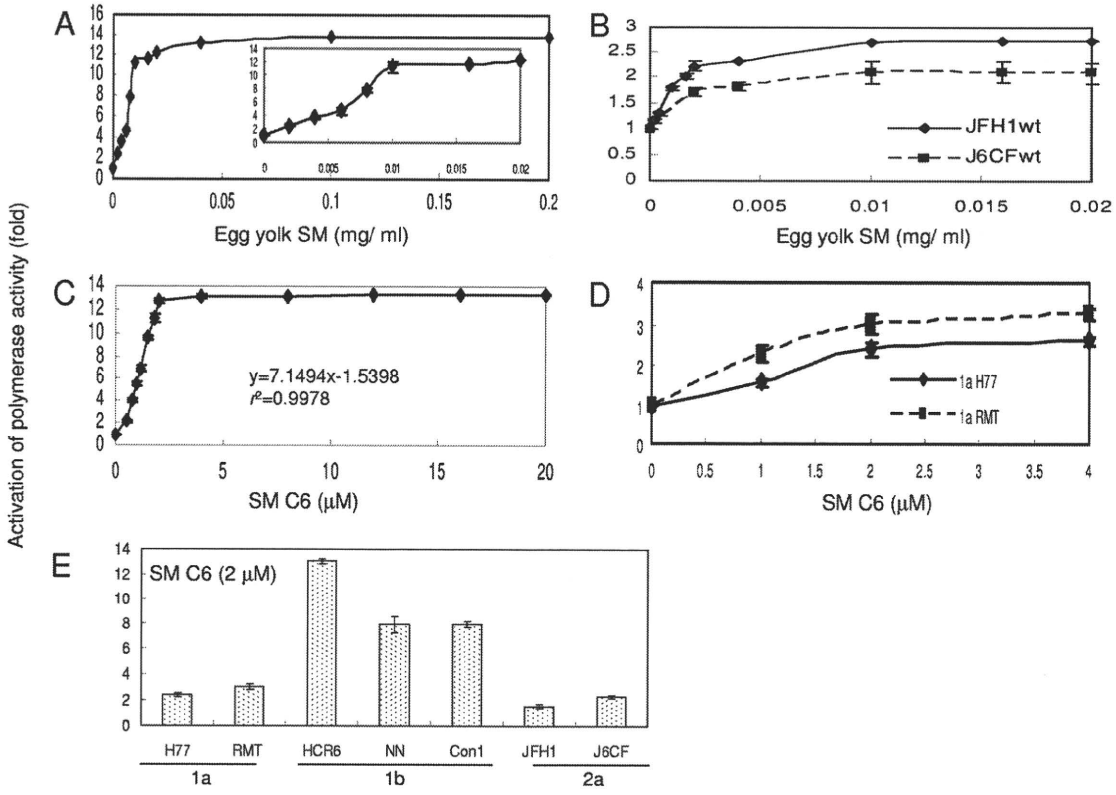

FIG. 1. Sphingomyelin activation of HCV RNA polymerases. (A) Activation kinetics of HCV HCR6 (1b) RdRp wt by egg yolk sphingomyelin (SM). The inset shows activation produced by 0 to 0.02 mg/ml egg yolk sphingomyelin. Activation kinetics of HCV 2a (JFH1 and J6CF) RdRps by egg yolk sphingomyelin (B) and of HCV HCR6 (1b) RdRp wt by hexanoyl sphingomyelin (SM C6) (C). In panel C, the first order of the graph was fitted by linear regression; the calculated equation is indicated in the graph. (D) Activation kinetics of HCV 1a (H77 and RMT) RdRps by hexanoyl sphingomyelin. (E) Activation effect of hexanoyl sphingomyelin on HCV RdRp of various genotypes. HCV RdRp (100 nM) was incubated with or without 2 μM SM C6. The names of the RdRps are indicated below the graph. Mean ± standard deviation of the activation ratio was calculated from three independent experiments.

RdRp wt, its activation kinetics were calculated using hexanoyl sphingomyelin (Fig. 1C, SM C6). The equation for the first-order ratio of hexanoyl sphingomyelin activation according to linear regression fitting was as follows: $y = 7.1494x - 1.5398$, where y is the activation ratio and x is the sphingomyelin concentration ($r^2 = 0.9978$). RdRp activation had almost plateaued at 2 μM hexanoyl sphingomyelin. The activation kinetics of JFH1 (2a) and J6CF (2a) RdRps in egg yolk sphingomyelin were biphasic and plateaued at 0.01 mg/ml. Those of RMT (1a) and H77 (1a) RdRps in hexanoyl sphingomyelin were also biphasic and plateaued at 2 μM. The curve of the first order was fitted by linear regression. The molar ratio of RdRp to hexanoyl sphingomyelin at its plateau was calculated as 1:20.

Because RdRp activation had almost plateaued at 2 μM hexanoyl sphingomyelin, we compared the effect of sphingomyelin on 100 M concentrations of RNA polymerases of the HCV 1a, 1b, and 2a genotypes using 2 μM hexanoyl sphingomyelin (Fig. 1E and Table 1).

Helix-turn-helix structure for sphingomyelin binding and activation. Sphingomyelin binds to the SBD peptide (see HCV SBD in Fig. 7) (29). Initially, we tested whether SBD was the sphingomyelin binding site in HCV RdRp by ELISA (Fig. 2A and Table 1). When the L245 and I253 residues of the SBD peptide were mutated to A, sphingomyelin binding activity was lost (29). We introduced the same mutations in HCV HCR6 (1b) RdRp and purified HCR6 (1b) RdRp with mutations L245A, I253A, and L245A/I253A. Because the C-terminal His-tagged HCR6 RdRp(L245A/I253A) was not soluble, it was solubilized by tagging of glutathione *S*-transferase (GST) sequence at the N terminus but lost polymerase activity. As the L245A/I253A mutant had lost its polymerase activity, polymerase activation was tested only for L245A and I253A (Fig. 2B and Table 1). These results confirmed that SBD located in the finger domain (residues 230E to 263G) successfully achieved sphingomyelin binding in HCV RdRp and that sphingomyelin did not bind to the SBD when the helix-turn-helix structure had been destroyed by the L245A or I253A mutation (29).

The sphingomyelin binding activities of genotype 1a and 2a RdRps were also tested (Fig. 2 and Table 1). Both JFH1 and J6CF were tested for genotype 2a because J6CF (2a) RdRp had an additional amino acid difference at position 241 in the SBD, and its sphingomyelin binding activity was very low (Fig. 2A and 7A; Table 1). J6CF (2a) RdRp(R241Q) showed the same sphingomyelin binding activity as HCR6 (1b) RdRp wt, indicating that 241Q was the critical amino acid for sphingomyelin binding. J6CF (2a) RdRp(S244D) and RdRp(R241Q/S244D) also showed higher sphingomyelin binding activity

TABLE 1. Summary of sphingomyelin activation of HCV RNA polymerase activities

Parameter	Value for the parameter by RdRp genotype, strain, and variant[a]																					
	1b								1a						2a							
	HCR6					NN	Con1	RMT	H77		J6CF				JFH1							
	wt	L245A	I253A	L245A/I253A	D244S	wt	wt	wt	wt	A238S/Q248E	wt	R241Q	S244D	R241Q/S244D	wt	A242C	S244D	A242C/S244D	T251Q
SM binding (%)[b]	100	24.3	30.8	15.5	78.7	93.4	117	144	86.7	82.5	19.3	118	53.1	80.2	70.4	75.5	93.1	92.4	80.7
Activation of polymerase (*n*-fold)[c]	13.0 (11.2)[d]	(2.8)[d]	(2.5)[d]	ND	3.6	7.9	7.9	3.0	2.0	8.1	2.3	4.3	5.6	3.4	1.6	1.0	3.1	4.4	1.8
Activation of RNA binding (*n*-fold)[c]	4.5	2.6	1.7	ND	1.9	ND	ND	ND	1.4	3.3	1.5	3.6	3.2	1.7	1.3	ND	ND	1.4	ND

[a] Numbers were averaged from three independent experiments. ND, not done.
[b] Egg yolk sphingomyelin (SM; 250 ng) was used.
[c] Hexanoyl sphingomyelin (2 μM) was used.
[d] Egg yolk sphingomyelin (0.01 mg/ml) was used.

than the wt ($P < 0.001$) but lower binding than the R241Q mutant. However, S244D showed higher RdRp activation than R241Q ($P < 0.005$), while the RdRp activation ratio of the double mutant (R241Q/S244D) was lower than that of S244D or R241Q, although all of them activated RdRp with sphingomyelin ($P < 0.005$) (Fig. 2A and C and Table 1). For JFH1, when the JFH1 RdRp SBD was modified (A242C/S244D) to allow it to bind with more sphingomyelin than the wt ($P < 0.005$), the mutant JFH1 RdRp(A242C/S244D) was activated more than the wt by sphingomyelin ($P < 0.005$) (Fig. 2A and C; Table 1). The sphingomyelin binding activity of JFH1 RdRp(T251Q) was 80.7% of that of HCR6 (1b), and its activation ratio was 1.8-fold. These results agree that SBD is both the sphingomyelin activation and binding domain and that the domains for these two activities are somehow different.

We determined which amino acid, 242C or 244D, enhanced sphingomyelin binding by comparing HCR6 (1b) and JFH1 (2a) RdRps. Sphingomyelin binding of HCR6 (1b) RdRp(D244S) was 79% of that of the wt ($P < 0.005$) (Fig. 2A and Table 1), and its activation by sphingomyelin was only 3.6-fold (Fig. 2C and Table 1). The sphingomyelin binding of JFH1 (2a) RdRp(A242C) and RdRp(S244D) increased to 75.5% and 93.1%, respectively, of HCR6 (1b) RdRp wt (Fig. 2A and Table 1). This was significantly higher than that of JFH1 (2a) RdRp wt ($P < 0.005$), and the sphingomyelin activation of JFH1 (2a) RdRp(A242C) and RdRp(S244D) was increased 1.0-fold and 3.1-fold, respectively ($P < 0.005$) (Fig. 2C and Table 1). From these mutation analyses of the J6CF and JFH1 RdRps, we concluded that 244D enhanced sphingomyelin binding and RdRp activation.

HCV 1a RdRps were not activated even though sphingomyelin bound to them (Fig. 1E and 2A and Table 1). We then tried to elucidate the domains responsible for sphingomyelin activation. There are 14 amino acids (residues 19, 25, 81, 111, 120, 131, 184, 270, 272, 329, 436, 464, 487, and 540) unique to genotype 1a RdRp in the region of residues 1 to 570 and two amino acid differences unique to 1a RdRp in SBD, i.e., 238A and 248Q (see Fig. 6A). Initially, we focused on the SBD and introduced the A238S and Q248E mutations into the H77 (2a) RdRp SBD (Fig. 2A and D and Table 1). The sphingomyelin binding activity of H77 (2a) RdRp(A238S/Q248E) was similar to that of H77 (2a) RdRp wt. The sphingomyelin activation ratio of H77 (2a) RdRp(A238S/Q248E) was increased 8.1-fold, leading us to conclude that these mutations are essential to sphingomyelin activation.

Effect of lipids on HCV RNA polymerase activity. In order to elucidate the structure of the lipids involved in activation of HCV RdRp, D-lactosyl-β-1,1′-*N*-octanoyl-D-*erythro*-sphingosine [C_8-lactosyl(β) ceramide], D-glucosyl-β1-17-N-octanoyl-D-*erythro*-sphingosine (C_8-β-D-glucosyl ceramide), *N*-hexanol-D-*erythro*-sphingosine (C_6-ceramide), and cholesterol were tested for their abilities to activate RdRp. The relative polymerase activities of 100 nM HCV HCR6 (1b) RdRp activated with 0.01 mg/ml egg yolk sphingomyelin, 2 μM hexanoyl sphingomyelin, 8 μM C_8-lactosyl(β) ceramide, 12 μM C_8-β-D-glucosyl ceramide, 12 μM C_6-ceramide, and 0.02 mg/ml cholesterol were 11.2, 13.0, 5.66, 4.19, 1.12, and 2.25 of that without lipids, respectively (Fig. 3A). The amount of lipids that gave the maximum activation was calculated from the kinetics of the lipids bound to HCR6 (1b) and JFH1 (2a) RdRps (Fig. 3B and

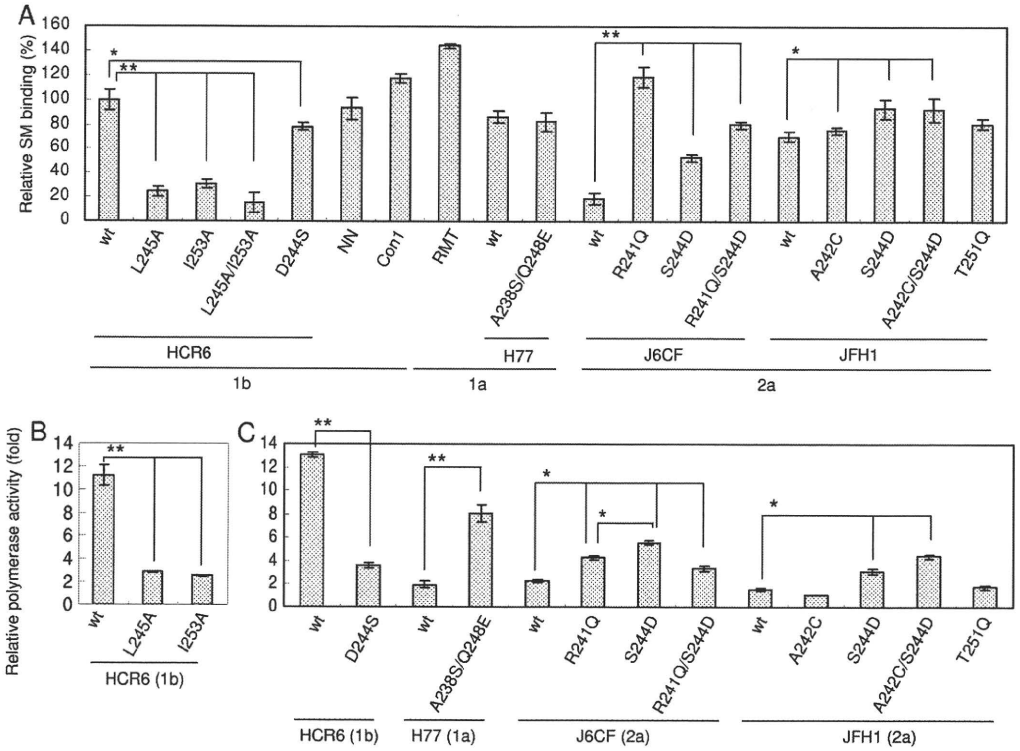

FIG. 2. Sphingomyelin binding and activation of HCV RNA polymerase sphingomyelin binding domain mutants. Names of RdRps are indicated below the graphs. (A) Egg yolk sphingomyelin (SM) binding activity relative to that of HCR6 (1b) RdRp wt. Mean ± standard deviation of the binding was calculated from three independent experiments. (B) Egg yolk sphingomyelin activation of HCR6 (1b) RdRps. RdRps (100 nM) were incubated with or without 0.01 mg/ml egg yolk sphingomyelin. (C) Hexanoyl sphingomyelin activation of the RdRps (RdRp names are indicated below the graphs). HCV RdRps (100 nM) were incubated with or without 2 μM hexanoyl sphingomyelin. The mean ± standard deviation of the activation ratio was calculated from three independent experiments. *, $P < 0.005$; ** $P < 0.001$.

C). C_8-lactosyl(β) ceramide and C_8-β-D-glucosyl ceramide activated HCR6 (1b) RdRp compared with the linear regression kinetics of the reaction with hexanoyl sphingomyelin as it plateaued (Fig. 1C and 3B). Cholesterol activated HCR6 (1b) RdRp slightly but did not activate JFH1 (2a) RdRp (Fig. 3C). We therefore concluded that the phosphocholine of sphingomyelin bound to the SBD of HCV RdRp because the order of HCV RdRp activation was hexanoyl sphingomyelin > C_8-lactosyl(β) ceramide > C_8-β-D-glucosyl ceramide, and C_6-ceramide did not activate HCV HCR6 (1b) RdRp. The polarity of the phosphocholine of sphingomyelin is important for HCV RdRp activation (see Fig. S5 in the supplemental material).

In order to test whether phosphocholine activated HCV RdRp (Fig. 3D), HCR6 (1b) RdRp was incubated with 0.4, 2, 20, 100, and 400 μg and 2, 4, 11, 54, and 100 mg of phosphocholine. Up to 400 μg of phosphocholine did not affect RdRp activity, but more than 2 mg of phosphocholine inhibited RdRp activity.

Effect of sphingomyelin on the template RNA binding of HCV RNA polymerase. The mechanism of HCV RdRp activation was analyzed. RNA polymerase changes its conformation throughout the different transcription steps, and template binding is the first step of transcription (9). Therefore, the effect of sphingomyelin on template RNA binding activity was tested (Fig. 4A and Table 1). Sphingomyelin enhanced the template RNA binding of HCR6 (1b) RdRp wt but not that of JFH1 (2a), H6CF (2a), or H77 (1a) wt RdRp. When the A238S/Q248E mutation was introduced into H77 (1a) RdRp, the RNA binding was enhanced. J6CF (2a) RdRp R241Q and S244D mutants showed similar enhancement of RNA binding, but the R241Q/S244D double mutant did not. The activation effect of RNA binding of HCR6 (1b) RdRp mutants L245A, I253A, and D244S was lower than that of RdRp wt. JFH1 (2a) RdRp wt and RdRp(A242C/S244D) showed similar RNA binding activation levels. Based on a comparison of the sphingomyelin activation of HCR6 (1b) RdRp wt and its mutants which lost sphingomyelin binding with J6CF (2a) RdRp wt and the R241Q and S244D mutants and H77 (1a) RdRp wt and the A238S/Q248E mutant, we concluded that polymerase activation by sphingomyelin was induced mainly via activation of the template RNA binding of RdRp. RNA binding activity of JFH1 (2a) RdRp wt and RdRp(A242C/S244D) was almost saturated because RNA binding of these RdRps was not activated by sphingomyelin (see Fig. S4 in the supplemental material).

HCV RdRp has to be bound with sphingomyelin before or at the same time as it binds to template RNA. After RdRp had bound to the template RNA, sphingomyelin did not enhance template RNA binding strongly (Fig. 4B).

Effect of the sphingomyelin binding domain mutations for HCV replicon activity with myriocin. In order to confirm sphingomyelin activation of HCV polymerase activity in a viral replication system, HCV replicon activity of the loss-of-function mutant HCV NN (1b) NS5B(D244S) and the gain-of-

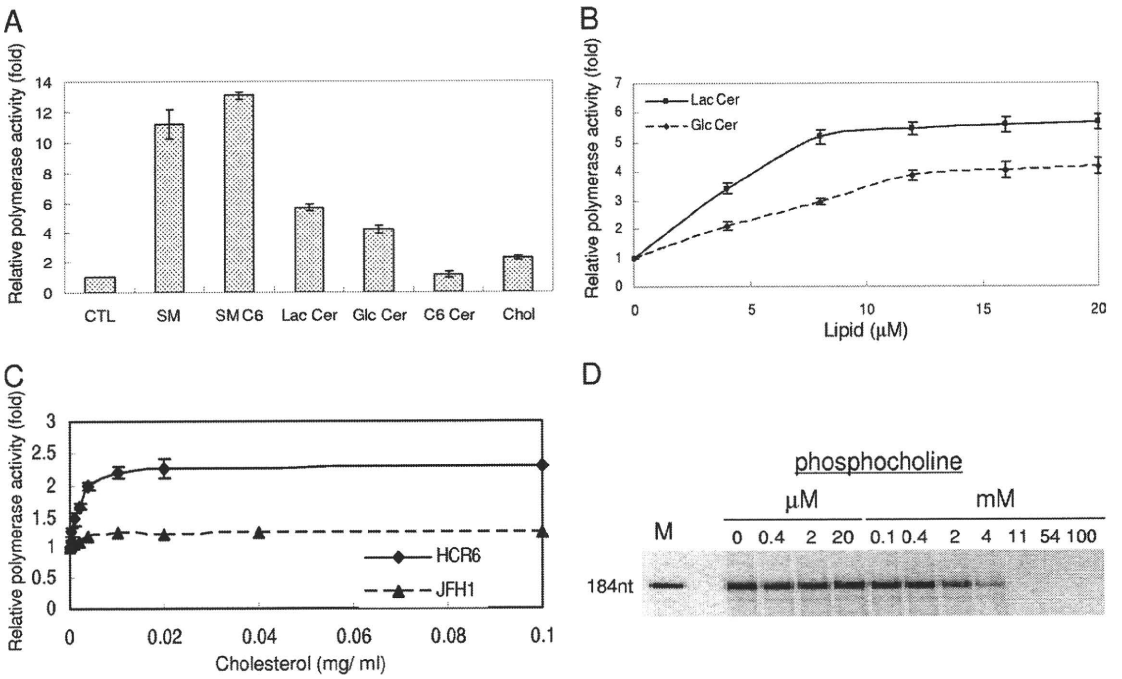

FIG. 3. HCV RNA polymerase activation effect of lipids. (A) Lipid activation of HCR6 (1b) RdRp wt. HCV HCR6 (1b) RdRp wt (100 nM) was incubated with or without (control [CTL]) 0.01 mg/ml egg yolk sphingomyelin (SM), 2 μM hexanoyl sphingomyelin (SM C6), 8 μM C_8-lactosyl(β) ceramide (Lac Cer), 12 μM C_8-β-D-glucosyl ceramide (Glc Cer), 12 μM C_6-ceramide (C6 Cer), or 0.02 mg/ml cholesterol (chol). (B) Activation kinetics of C_8-lactosyl(β) ceramide (Lac Cer) and C_8-β-D-glucosyl ceramide (Glc Cer) on HCR6 (1) RdRp. (C) Activation kinetics of cholesterol on HCR6 (1b) and JFH1 (12a) RdRps. (D) The effect of phosphocholine on HCR6 (1b) RdRp. The mean ± standard deviation of the activation ratio was calculated from three independent experiments.

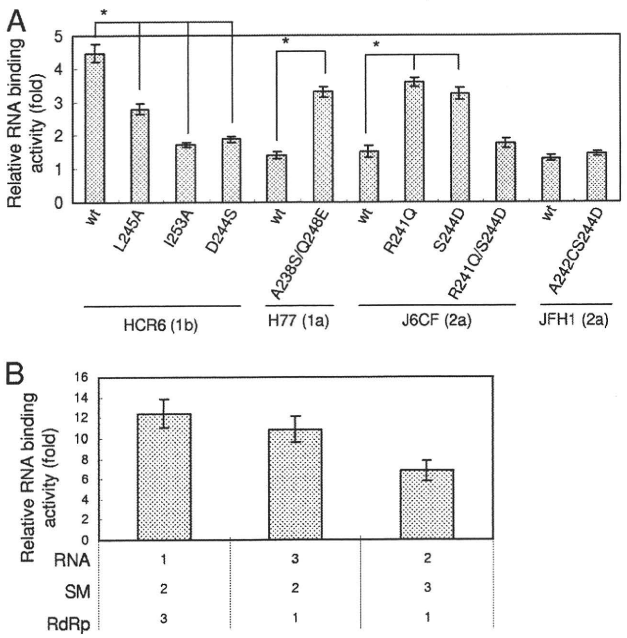

FIG. 4. Sphingomyelin activation of the RNA binding activity of HCV RNA polymerase. (A) Sphingomyelin activation of RNA filter binding of HCV RdRps (RdRp names are indicated below the graph). RdRps and ^{32}P-labeled RNA template (SL12-1S) were incubated with or without egg yolk sphingomyelin (SM), before filtration. (B) Effect of the order of sphingomyelin treatment. Numbers below the graph indicate the order in which the reagents were added. The graph represents the ratio to RNA binding without sphingomyelin. The mean ± standard deviation of the activation ratio was calculated from three independent experiments. *, $P < 0.01$.

function mutants H77 (1a) NS5B(A238S/Q248E) and JFH1 (2a) NS5B(A242C/S244D) were compared with 5 and 50 nM myriocin treatment for 72 h (Fig. 5).

First, HCV replicon activity was compared as the relative luciferase activity (Fig. 5A). Both JFH1 (2a) wt and NS5B(A242C/S244D) replicons showed similar and strong replicon activity ($133 \times 10^3 \pm 12 \times 10^3$ and $138 \times 10^3 \pm 8.5 \times 10^3$, respectively). JFH1 (2a) wt replicon was resistant to myriocin treatment, as reported by Aizaki et al. using other SPT inhibitors (3). The JFH1 (2a) NS5B(A242C/S244D) replicon became sensitive to myriocin but still showed higher replicon activity than NN (1b) or H77 (1a) replicons even at 50 nM myriocin.

To analyze the effect of mutations precisely, the replicon activity relative to each wt strain was compared (Fig. 5B). The JFH1 (2a) wt replicon with 50 nM myriocin showed the same luciferase activity as the wt without myriocin (102% ± 9.6%). JFH1 (2a) NS5B(A242C/S244D) replicon activity was the same as that of the wt without myriocin (103% ± 12%); with 5 nM myriocin it was 84.1% ± 6.6% of the wt level, but with 50 nM myriocin it was 70.3% ± 5.3% of the wt level, which was significantly lower ($P < 0.01$). NN (1b) wt replicon activity was 45.3% ± 6.6% with 5 nM myriocin and 21.7% ± 2.9% with 50 nM myriocin relative to the wt level without myriocin. NN (1b) NS5B(D244S) replicon activity was 72.2% ± 12% without myriocin ($P < 0.05$), 44.0% ± 7.4% with 5 nM myriocin, and 38.1% ± 4.2% with 50 nM myriocin relative to wt level without myriocin, which was significantly higher ($P < 0.01$). Thus, NN (1b) NS5B(D244S) showed lower replicon activity than the wt

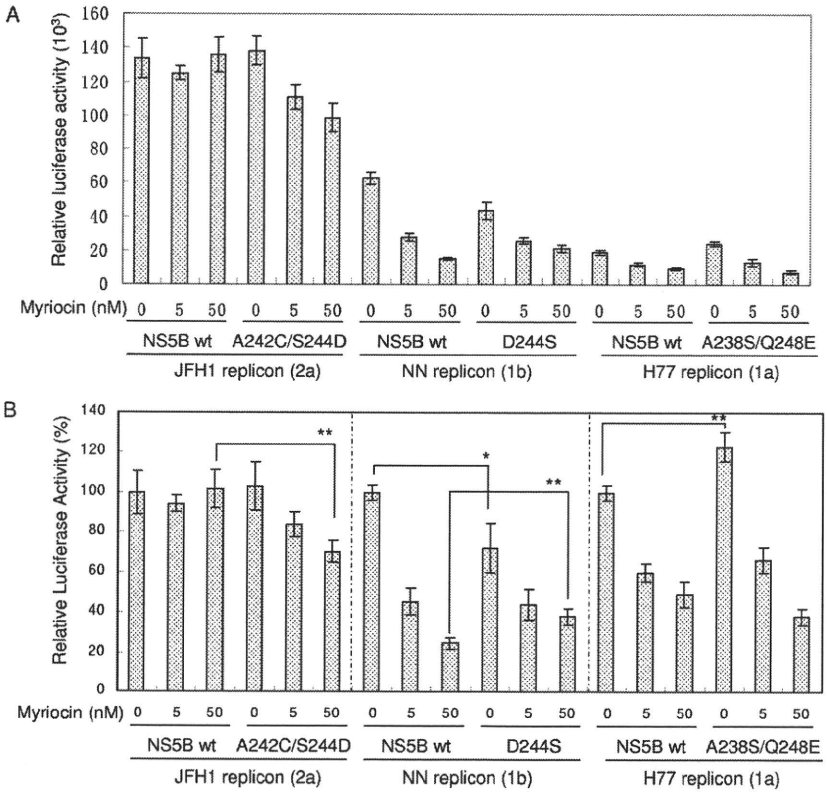

FIG. 5. Myriocin inhibition of HCV replicon activity. Huh7.5.1 cells were incubated with myriocin after transfection with the HCV replicons indicated below the graphs. Means ± standard deviations of the relative luciferase activity at 72 h after myriocin treatment compared to activity at 4 h after transfection (A) and to that of each wt without myriocin (B) were calculated from three independent measurements. *, $P < 0.05$; ** $P < 0.01$.

and was less sensitive to myriocin than the wt. H77 (1a) wt replicon activity was 59.9% ± 4.2% with 5 nM myriocin and 49.2% ± 6.4% with 50 nM myriocin relative to the wt level without myriocin. H77 (1a) NS5B(A238S/Q248E) replicon activity was 123% ± 7.1% without myriocin ($P < 0.01$), 66.1% ± 6.3% with 5 nM myriocin, and 38.0% ± 4.1% with 50 nM myriocin relative to wt level without myriocin. Both H77 (1a) wt and NS5B(A238S/Q248E) replicons were sensitive to myriocin, and the replicon activity of NS5B(A238S/Q248E) was higher than that of the wt.

JFH1 (2a) RdRp(A242C/S244D) localized in the DRM fractions. Myriocin sensitivity of JFH1 (2a) NS5B(A242C/S244D) replicon indicates the importance of 244D in JFH1 NS5B for sphingomyelin binding. To further confirm the role of 244D for recruitment of HCV RdRp to the detergent-resistant membrane (DRM), where the HCV replication complex exists, we compared the distribution of NS5A and NS5B of JFH1 (2a) wt and NS5B(A242C/S244D) in their replicon cells by sucrose density gradient centrifugation of the DRM (Fig. 6). NS5A proteins of both JFH1 (2a) wt and NS5B(A242C/S244D) replicons localized in the DRM fraction where caveolin-2 was present (11, 27), but most of NS5B wt localized in the Triton-soluble fractions. NS5B of JFH1 (2a) NS5B(A242C/S244D) replicon was shifted to the DRM fraction from the soluble fraction. The shift of NS5B(A242C/S244D) localization into the DRM demonstrated that SBD was the DRM localization domain of NS5B and that residue 244D was important for this localization.

DISCUSSION

Hepatitis C virus is an envelope virus, and the lipid components of the virion play important roles in HCV infectivity and virion assembly (3, 15, 20, 24). HCV replication complexes localize in lipid raft structures/DRMs in the membrane frac-

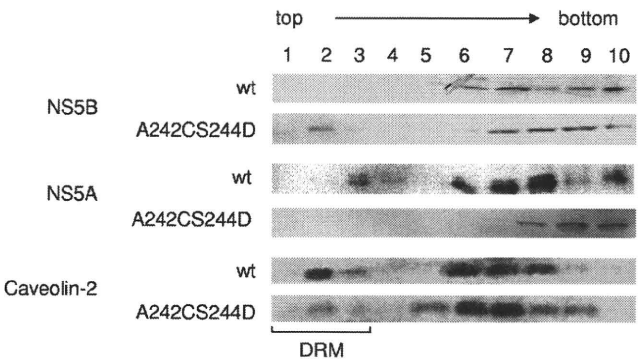

FIG. 6. Membrane floating assay of JFH1 wt and NS5B(A242C/S244D) replicon cells. The PNS fractions of HCV JFH1 (2a) wt and NS5B(A242C/S244D) replicon cells were treated with 1% Triton X-100 in TNE buffer for 30 min at 4°C and subjected to 10 to 40% sucrose gradient centrifugation in TNE buffer. Each fraction was subjected to 10% SDS-PAGE, followed by Western blotting with anti-NS5A, -NS5B, and -caveolin-2 antibodies. Fractions are numbered as indicated at the top of the panel. The DRM fractions (fractions 1 to 3) are indicated.

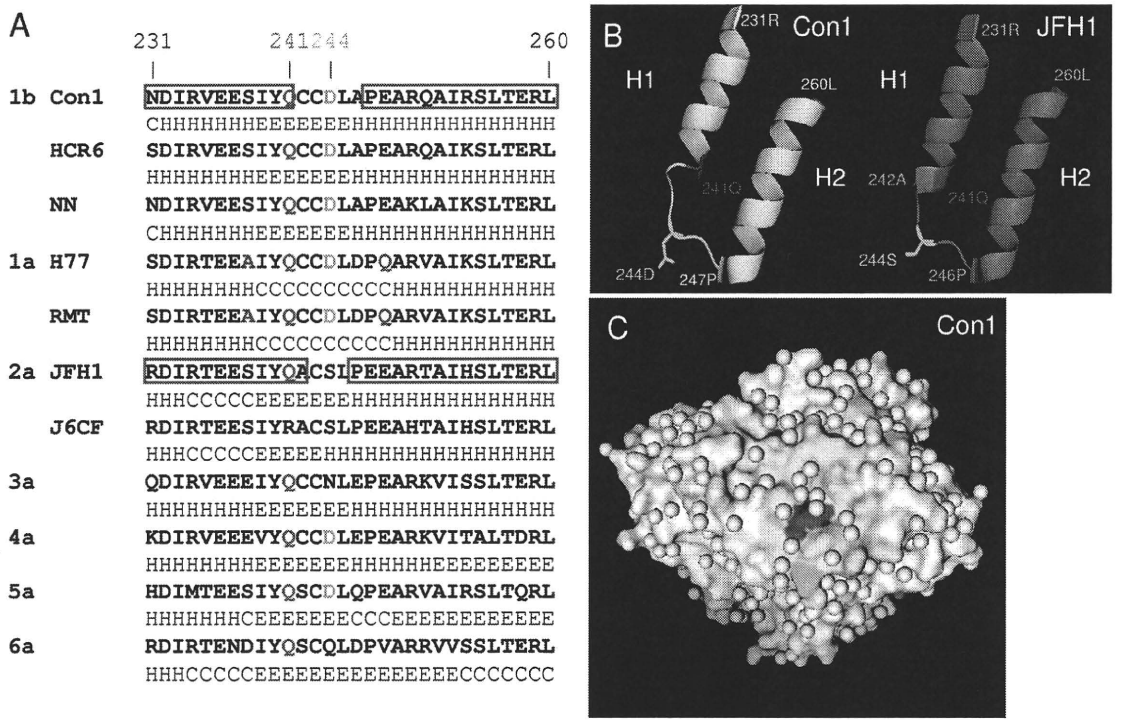

FIG. 7. Sphingomyelin binding domain (SBD) of HCV RNA polymerase. (A) The SBDs (231N to 260L) of HCV RdRps are aligned together with their secondary structure predicted by the Chou-Fasman program (10). The predicted secondary structure is indicated below the sequence as follows: H, α-helix; E, β-sheet; and C, coil. The α-helix structures of HCV Con1 (1b) RdRp and JFH1 (2a) RdRp are boxed in red. Residues 241Q and 244D are indicated in red and green, respectively. The 238A and 248E of the H77 and RMT (1a) RdRps are indicated in purple. GenBank accession numbers of HCV genotypes 3a, 4a, 5a, and 6a are GU814263 (12), GU814265 (12), Y13184 (8), and Y12083 (1), respectively. (B) Comparison of the SBDs of HCV Con1 (1b) (yellow) and JFH1 (2a) RdRps (magenta). The starting and ending amino acids of H1 and H2 are indicated. The sphingomyelin binding site, 241Q, is indicated in red, and 244D of Con1 (1b) and 244S of JFH1 (2a) RdRp are indicated in green. (C) Surface model of HCV Con1 (1b) RdRp. SBD is indicated in yellow, and 241Q and 244D are indicated in red and green, respectively. The structures of the Con1 and JFH1 RdRps were constructed by PyMOL, version 1.1.1 (http://www.pymol.org/). PDB numbers of Con1 (1b) RdRp and JFH1 (2a) RdRp are 3FQL (14) and 3I5K (31), respectively.

tions of subgenomic replicon cells (30). Lipid rafts are composed mainly of sphingomyelin, cholesterol, and glycosphingolipids. Most reports regarding the relationship between lipids and HCV have examined virion assembly, infectivity, and the localization of HCV, but their biochemical interactions have not been reported. Our findings clearly demonstrate that sphingomyelin plays an important role not only in HCV replication complex formation and its localization but also in HCV RdRp activity.

The helix-turn-helix structure of the SBD (residues 230 to 263), which is located between RNA polymerase motifs A and B, has been proposed as the sphingomyelin binding domain of HCV RdRp (29). We compared the SBD of Con1 (1b) (Protein Data Bank [PDB] 3FQL) (14) and JFH1 (2a) (PDB 3I5K) (31) and the secondary structure of the amino acids (201 to 290) in the SBD predicted by the Chou-Fasman program (10) (Fig. 7; see also Fig. S5 in the supplemental material) because the helix structures of the SBD of Con1 (helix 1 [H1], 231N to 241Q; helix 2 [H2], 247A to 260L) and JFH1 (H1, 231R to 242A; H2, 246P to 260L) RdRp fit with those predicted by the Chou-Fasman program. The structures contributing to sphingomyelin binding and activation are H1 and H2 and the junction (turn) between the two helix structures that are similar to the human immunodeficiency virus (HIV) gp120 V3 domain, prion protein (PrP), and β-amyloid peptide (13, 22). Although Con1 (1b) RdRp has a shorter helix structure than JFH1 (2a) RdRp (Fig. 6B), the structures of their SBDs are very similar (Fig. 7; see also Fig. S5). When the helix-turn-helix structure of the SBD was destroyed (HCR6 genotype 1b RdRp mutants L245A and I253A), the RdRp lost sphingomyelin binding activity and lost its activation (Fig. 2).

In order to study the structure-function relationship of the SBD and sphingomyelin, we compared the SBD of genotype 1a, 1b and 2a RdRps and particularly focused on residue 244D in the turn and residues 241Q and 238S/248E in the helix domains. The polar amino acid 241Q and the negatively charged 244D of Con1 (1b) RdRp located on the surface of the RdRp molecule bind and interact with the positively charged choline residue of sphingomyelin (Fig. 7C; see also Fig. S5 in the supplemental material). The positively charged 241R repels the choline residue of sphingomyelin, and as a result, J6CF (a) RdRp wt did not bind to sphingomyelin. J6CF (2a) RdRp(R241Q) showed almost the same sphingomyelin binding activity as HCR6 (1b) RdRp wt. This ionic interaction between SBD and sphingomyelin agrees with the activation of lipids with different sphingosine structures and fatty acid chains (Fig. 3A). JFH1 (2a) RdRp does not interact well with sphingomyelin because it does not have the negatively charged

amino acids at the tip of its turn structure. Once its 244S was changed to D, more sphingomyelin bound to JFH1 (2a) RdRp and activated the RdRp (Fig. 2A and C). The reason for the low activation of J6CF (2a) RdRp(R241Q/S244D) is not clear. Sometimes mutations affect the entire conformation of the molecule. In conclusion, from the comparison of sphingomyelin binding and activation of HCR6 (1b), J6CF (2a), and JFH1 (2a) RdRp SBD mutants, 241Q is the essential amino acid for sphingomyelin binding in the SBD. Amino acid 244D enhanced both binding and RdRp activation.

The *in vitro* sphingomyelin binding and RdRp activation experiments indicate that sphingomyelin binding and its RdRp activation are different biochemical reactions because we found controversial activation rates for sphingomyelin binding and RdRp activation among J6CF (2a) RdRp mutants (Fig. 2). The relationship between sphingomyelin binding and the activation of polymerase activity was studied by comparing genotype 1b and 1a RdRps, both of which bind to sphingomyelin (Fig. 2). However, 1a RdRp is not activated by sphingomyelin because both of the helix structures of 1a RdRp are probably terminated at 238A and 248Q, making its helix structures shorter than those of 1b RdRp (Fig. 6A). The length of the helix structure may be essential for sphingomyelin activation because RdRp changes its structure to bind to template RNA when sphingomyelin binds to SBD (Fig. 4).

HCV RdRp changes its conformations at the early stages of transcription initiation, including the template RNA binding step (6, 9). Sphingomyelin binding is likely to change the conformation of 1b RdRp to recruit template RNA and initiate transcription efficiently. Comparison of the activation ratio of RNA binding and polymerase activity of 1b RdRp, J6CF (2a) RdRp wt and R241Q and S244D mutants, and JFH1 (2a) RdRp wt and mutant A242C/S244D suggests that steps other than RNA binding are also likely to be activated by sphingomyelin.

From a kinetic analysis of sphingomyelin activation (Fig. 1C and D), 20 sphingomyelin molecules are estimated to interact with the SBD of RdRp and activate it because sphingomyelin activation plateaued at 20 sphingomyelin molecules per HCV RdRp molecule. It is not clear whether 20 sphingomyelin molecules form a micelle or a layer structure. However, the structure of sphingomyelin is important for the activation of HCV RdRp because phosphocholine did not activate the RdRp (Fig. 3D).

To confirm these biochemical findings in HCV replication, we tested the effect of SBD mutations in HCV replicon systems with the SPT inhibitor myriocin (Fig. 5) (4, 33) because NA255 was not available. The loss-of-function mutant, HCV NN (1b) NS5B(D244S), showed lower replicon activity than NN (1b) wt and more resistance to 50 nM myriocin, which did not affect the viability of cells (4, 33), than the wt. The gain-of-function mutant, H77 (1a) NS5B(A238S/Q248E), showed higher replicon activity than H77 wt and retained myriocin sensitivity because it had the sphingomyelin binding sites 241Q and 244D. At 50 nM myriocin, another gain-of-function mutant, JFH1 (2a) NS5B(A242C/S244D), was inhibited although its activity was the same as that of JFH1 (2a) wt without myriocin because the JFH1 wt replicon had high replicon activity without myriocin (Fig. 5A). The JFH1 replicon activity may be maximal in the system; therefore, the JFH1 (2a) NS5B(A242C/S244D) replicon did not show higher activity than JFH1 (2a) wt without myriocin while H77 (1a) NS5B(A238S/Q248E) showed higher replicon activity than H77 wt.

The binding and RdRp activation activity of the amino acid 244 mutants by sphingomyelin did not differ greatly from the wt *in vitro*. However, the myriocin sensitivity of JFH1 (2a) NS5B(S244D) was demonstrated clearly. That of H77 (1a) NS5B(A238S/Q248E) indicated that sphingomyelin binding was the target of myriocin inhibition, not the sphingomyelin activation of RdRp. These data confirm the importance of 241Q, 244D, and the helix structure in SBD for HCV replication in the cells.

Sphingomyelin is the major component of the lipid raft structure/DRM where the HCV genome replicates. To confirm that the SBD is the membrane binding site of HCV RdRp, we analyzed the localization of NS5B of JFH1 (2a) wt and NS5B(A242C/S244D) replicons by membrane floating assay (Fig. 6). JFH1 (2a) NS5B wt did not localize in the DRM. However, the localization of NS5B of the JFH1 (2a) NS5B(A242C/S244D) replicon shifted to the DRM from the soluble fractions. Previously, HCV NS5B was believed to localize in the DRM by its C-terminal hydrophobic sequences (21). However, our data demonstrate that the SBD is the membrane localization domain of HCV NS5B, which agrees with the myriocin sensitivity of JFH1 (2a) NS5B(A242C/S244D) replicons (Fig. 5) and the release of HCV 1b NS5B from the DRM by another SPT inhibitor, NA255 (29).

This is the first report of RNA polymerase activation by lipids. Twenty sphingomyelin molecules interact with SBD, particularly with residues 241Q and 244D of HCV (1b) RdRp, and change the conformation of the RdRp in order to recruit RNA templates. At the same time, HCV RdRp molecules may be aligned on the sphingomyelin layer formed via interactions between the hydrocarbon chains of sphingosine and fatty acids via placement of their SBD into the layer (Fig. 7C). Consistent with previous research (3, 23, 37), our findings explain why the inhibitors of the sphingolipid biosynthetic pathway influence subgenomic replicons derived from HCV genotypes 1a and 1b but not those derived from JFH1 (2a) (Fig. 5). Most HCV isolates have 241Q in NS5B, and some of them also have 244D (Fig. 7A). These sphingomyelin interactions are new targets for the treatment of HCV.

ACKNOWLEDGMENTS

We thank C. Rice and R. Bartenshlager for the HCV H77 and Con1 plasmids, respectively. We also thank F. Chisari for Huh7.5.1 and Huh7/src cells.

This work was supported by a grant-in-aid from the Chinese Academy of Sciences (O514P51131 and KSCX1-YW-10), the Chinese 973 project (2009CB522504), and the Chinese National Science and Technology Major Project (2008ZX10002-014).

REFERENCES

1. **Adams, N. J., R. W. Chamberlain, L. A. Taylor, F. Davidson, C. K. Lin, R. M. Elliott, and P. Simmonds.** 1997. Complete coding sequence of hepatitis C virus genotype 6a. Biochem. Biophys. Res. Commun. **234**:393–396.
2. **Aizaki, H., K. J. Lee, V. M. Sung, H. Ishiko, and M. M. Lai.** 2004. Characterization of the hepatitis C virus RNA replication complex associated with lipid rafts. Virology **324**:450–461.
3. **Aizaki, H., K. Morikawa, M. Fukasawa, H. Hara, Y. Inoue, H. Tani, K. Saito, M. Nishijima, K. Hanada, Y. Matsuura, M. M. Lai, T. Miyamura, T. Wakita, and T. Suzuki.** 2008. Critical role of virion-associated cholesterol and sphingolipid in hepatitis C virus infection. J. Virol. **82**:5715–5724.
4. **Amemiya, F., S. Maekawa, Y. Itakura, A. Kanayama, A. Matsui, S. Takano, T. Yamaguchi, J. Itakura, T. Kitamura, T. Inoue, M. Sakamoto, K. Yamau-**

chi, S. Okada, A. Yamashita, N. Sakamoto, M. Itoh, and N. Enomoto. 2008. Targeting lipid metabolism in the treatment of hepatitis C virus infection. J. Infect. Dis. **197:**361–370.

5. **Binder, M., D. Quinkert, O. Bochkarova, R. Klein, N. Kezmic, R. Bartenschlager, and V. Lohmann.** 2007. Identification of determinants involved in initiation of hepatitis C virus RNA synthesis by using intergenotypic replicase chimeras. J. Virol. **81:**5270–5283.
6. **Biswal, B. K., M. M. Cherney, M. Wang, L. Chan, C. G. Yannopoulos, D. Bilimoria, O. Nicolas, J. Bedard, and M. N. James.** 2005. Crystal structures of the RNA-dependent RNA polymerase genotype 2a of hepatitis C virus reveal two conformations and suggest mechanisms of inhibition by non-nucleoside inhibitors. J. Biol. Chem. **280:**18202–18210.
7. **Blight, K. J., J. A. McKeating, J. Marcotrigiano, and C. M. Rice.** 2003. Efficient replication of hepatitis C virus genotype 1a RNAs in cell culture. J. Virol. **77:**3181–3190.
8. **Chamberlain, R. W., N. J. Adams, L. A. Taylor, P. Simmonds, and R. M. Elliott.** 1997. The complete coding sequence of hepatitis C virus genotype 5a, the predominant genotype in South Africa. Biochem. Biophys. Res. Commun. **236:**44–49.
9. **Chinnaswamy, S., I. Yarbrough, S. Palaninathan, C. T. Kumar, V. Vijayaraghavan, B. Demeler, S. M. Lemon, J. C. Sacchettini, and C. C. Kao.** 2008. A locking mechanism regulates RNA synthesis and host protein interaction by the hepatitis C virus polymerase. J. Biol. Chem. **283:**20535–20546.
10. **Chou, P. Y., and G. D. Fasman.** 1974. Prediction of protein conformation. Biochemistry **13:**222–245.
11. **Fujimoto, T., H. Kogo, K. Ishiguro, K. Tauchi, and R. Nomura.** 2001. Caveolin-2 is targeted to lipid droplets, a new "membrane domain" in the cell. J. Cell Biol. **152:**1079–1085.
12. **Gottwein, J. M., T. K. Scheel, B. Callendret, Y. P. Li, H. B. Eccleston, R. E. Engle, S. Govindarajan, W. Satterfield, R. H. Purcell, C. M. Walker, and J. Bukh.** Novel infectious cDNA clones of hepatitis C virus genotype 3a (strain S52) and 4a (strain ED43): genetic analyses and *in vivo* pathogenesis studies. J. Virol. **84:**5277–5293.
13. **Hammache, D., G. Pieroni, N. Yahi, O. Delezay, N. Koch, H. Lafont, C. Tamalet, and J. Fantini.** 1998. Specific interaction of HIV-1 and HIV-2 surface envelope glycoproteins with monolayers of galactosylceramide and ganglioside GM3. J. Biol. Chem. **273:**7967–7971.
14. **Hang, J. Q., Y. Yang, S. F. Harris, V. Leveque, H. J. Whittington, S. Rajyaguru, G. Ao-Ieong, M. F. McCown, A. Wong, A. M. Giannetti, S. Le Pogam, F. Talamas, N. Cammack, I. Najera, and K. Klumpp.** 2009. Slow binding inhibition and mechanism of resistance of non-nucleoside polymerase inhibitors of hepatitis C virus. J. Biol. Chem. **284:**15517–15529.
15. **Huang, H., F. Sun, D. M. Owen, W. Li, Y. Chen, M. Gale, Jr., and J. Ye.** 2007. Hepatitis C virus production by human hepatocytes dependent on assembly and secretion of very low-density lipoproteins. Proc. Natl. Acad. Sci. U. S. A. **104:**5848–5853.
16. **Ishii, N., K. Watashi, T. Hishiki, K. Goto, D. Inoue, M. Hijikata, T. Wakita, N. Kato, and K. Shimotohno.** 2006. Diverse effects of cyclosporine on hepatitis C virus strain replication. J. Virol. **80:**4510–4520.
17. **Kashiwagi, T., K. Hara, M. Kohara, K. Kohara, J. Iwahashi, N. Hamada, H. Yoshino, and T. Toyoda.** 2002. Kinetic analysis of C-terminally truncated RNA-dependent RNA polymerase of hepatitis C virus. Biochem. Biophys. Res. Commun. **290:**1188–1194.
18. **Kato, T., T. Date, M. Miyamoto, A. Furusaka, K. Tokushige, M. Mizokami, and T. Wakita.** 2003. Efficient replication of the genotype 2a hepatitis C virus subgenomic replicon. Gastroenterology **125:**1808–1817.
19. **Kiyosawa, K., T. Sodeyama, E. Tanaka, Y. Gibo, K. Yoshizawa, Y. Nakano, S. Furuta, Y. Akahane, K. Nishioka, R. H. Purcell, et al.** 1990. Interrelationship of blood transfusion, non-A, non-B hepatitis and hepatocellular carcinoma: analysis by detection of antibody to hepatitis C virus. Hepatology **12:**671–675.
20. **Lambot, M., S. Fretier, A. Op De Beeck, B. Quatannens, S. Lestavel, V. Clavey, and J. Dubuisson.** 2002. Reconstitution of hepatitis C virus envelope glycoproteins into liposomes as a surrogate model to study virus attachment. J. Biol. Chem. **277:**20625–20630.
21. **Lemon, S., C. Walker, M. Alter, and M. Yi.** 2007. Hepatitis C virus, p. 1253–1304. *In* D. M. Knipe, P. M. Howley, D. E. Griffin, R. A. Lamb, M. A. Martin, B. Roizman, and S. E. Straus (ed.), Fields virology, 5th ed. Lippincott Williams & Wilkins, Philadelphia, PA.
22. **Mahfoud, R., N. Garmy, M. Maresca, N. Yahi, A. Puigserver, and J. Fantini.** 2002. Identification of a common sphingolipid-binding domain in Alzheimer, prion, and HIV-1 proteins. J. Biol. Chem. **277:**11292–11296.
23. **Miyake, Y., Y. Kozutsumi, S. Nakamura, T. Fujita, and T. Kawasaki.** 1995. Serine palmitoyltransferase is the primary target of a sphingosine-like immunosuppressant, ISP-1/myriocin. Biochem. Biophys. Res. Commun. **211:** 396–403.
24. **Miyanari, Y., K. Atsuzawa, N. Usuda, K. Watashi, T. Hishiki, M. Zayas, R. Bartenschlager, T. Wakita, M. Hijikata, and K. Shimotohno.** 2007. The lipid droplet is an important organelle for hepatitis C virus production. Nat. Cell Biol. **9:**1089–1097.
25. **Murayama, A., T. Date, K. Morikawa, D. Akazawa, M. Miyamoto, M. Kaga, K. Ishii, T. Suzuki, T. Kato, M. Mizokami, and T. Wakita.** 2007. The NS3 helicase and NS5B-to-3′X regions are important for efficient hepatitis C virus strain JFH-1 replication in Huh7 cells. J. Virol. **81:**8030–8040.
26. **Murayama, A., L. Weng, T. Date, D. Akazawa, X. Tian, T. Suzuki, T. Kato, Y. Tanaka, M. Mizokami, T. Wakita, and T. Toyoda.** 2010. RNA polymerase activity and specific RNA structure are required for efficient HCV replication in cultured cells. PLoS Pathog. **6:**e1000885.
27. **Ostermeyer, A. G., J. M. Paci, Y. Zeng, D. M. Lublin, S. Munro, and D. A. Brown.** 2001. Accumulation of caveolin in the endoplasmic reticulum redirects the protein to lipid storage droplets. J. Cell Biol. **152:**1071–1078.
28. **Saito, I., T. Miyamura, A. Ohbayashi, H. Harada, T. Katayama, S. Kikuchi, Y. Watanabe, S. Koi, M. Onji, Y. Ohta, et al.** 1990. Hepatitis C virus infection is associated with the development of hepatocellular carcinoma. Proc. Natl. Acad. Sci. U. S. A. **87:**6547–6549.
29. **Sakamoto, H., K. Okamoto, M. Aoki, H. Kato, A. Katsume, A. Ohta, T. Tsukuda, N. Shimma, Y. Aoki, M. Arisawa, M. Kohara, and M. Sudoh.** 2005. Host sphingolipid biosynthesis as a target for hepatitis C virus therapy. Nat. Chem. Biol. **1:**333–337.
30. **Shi, S. T., K. J. Lee, H. Aizaki, S. B. Hwang, and M. M. Lai.** 2003. Hepatitis C virus RNA replication occurs on a detergent-resistant membrane that cofractionates with caveolin-2. J. Virol. **77:**4160–4168.
31. **Simister, P., M. Schmitt, M. Geitmann, O. Wicht, U. H. Danielson, R. Klein, S. Bressanelli, and V. Lohmann.** 2009. Structural and functional analysis of hepatitis C virus strain JFH1 polymerase. J. Virol. **83:**11926–11939.
32. **Tsukiyama-Kohara, K., S. Tone, I. Maruyama, K. Inoue, A. Katsume, H. Nuriya, H. Ohmori, J. Ohkawa, K. Taira, Y. Hoshikawa, F. Shibasaki, M. Reth, Y. Minatogawa, and M. Kohara.** 2004. Activation of the CKI-CDK-Rb-E2F pathway in full genome hepatitis C virus-expressing cells. J. Biol. Chem. **279:**14531–14541.
33. **Umehara, T., M. Sudoh, F. Yasui, C. Matsuda, Y. Hayashi, K. Chayama, and M. Kohara.** 2006. Serine palmitoyltransferase inhibitor suppresses HCV replication in a mouse model. Biochem. Biophys. Res. Commun. **346:**67–73.
34. **Wasley, A., and M. J. Alter.** 2000. Epidemiology of hepatitis C: geographic differences and temporal trends. Semin. Liver Dis. **20:**1–16.
35. **Watashi, K., N. Ishii, M. Hijikata, D. Inoue, T. Murata, Y. Miyanari, and K. Shimotohno.** 2005. Cyclophilin B is a functional regulator of hepatitis C virus RNA polymerase. Mol. Cell **19:**111–122.
36. **Weng, L., J. Du, J. Zhou, J. Ding, T. Wakita, M. Kohara, and T. Toyoda.** 2009. Modification of hepatitis C virus 1b RNA polymerase to make a highly active JFH1-type polymerase by mutation of the thumb domain. Arch. Virol. **154:**765–773.
37. **Yasuda, S., H. Kitagawa, M. Ueno, H. Ishitani, M. Fukasawa, M. Nishijima, S. Kobayashi, and K. Hanada.** 2001. A novel inhibitor of ceramide trafficking from the endoplasmic reticulum to the site of sphingomyelin synthesis. J. Biol. Chem. **276:**43994–44002.
38. **Zhong, J., P. Gastaminza, G. Cheng, S. Kapadia, T. Kato, D. R. Burton, S. F. Wieland, S. L. Uprichard, T. Wakita, and F. V. Chisari.** 2005. Robust hepatitis C virus infection in vitro. Proc. Natl. Acad. Sci. U. S. A. **102:**9294–9299.